8962 *Inorg. Chem.* **2010**, *49*, 8962–8976
DOI: 10.1021/ic101261f

Inorganic Chemistry
Article

Chemistry of the Oxophosphinidene Ligand. 1. Electronic Structure of the Anionic Complexes $[MCp\{P(O)R^*\}(CO)_2]^-$ (M = Mo, W; R* = 2,4,6-$C_6H_2{}^tBu_3$) and Their Reactions with H^+ and C-Based Electrophiles.

María Alonso, M. Angeles Alvarez, M. Esther García,* Daniel García-Vivó, and Miguel A. Ruiz*

Departamento de Química Orgánica e Inorgánica/IUQOEM, Universidad de Oviedo, 33071 Oviedo, Spain

Received June 24, 2010

The anionic phosphide-bridged complexes (H-DBU)$[M_2Cp_2(\mu\text{-}PHR^*)(CO)_4]$ (M = Mo, W; R* = 2,4,6-$C_6H_2{}^tBu_3$; Cp = η^5-C_5H_5, DBU = 1,8-diazabicyclo [5.4.0] undec-7-ene) react with molecular oxygen to give the corresponding oxophosphinidene complexes (H-DBU)$[MCp\{P(O)R^*\}(CO)_2]$ as major products (Mo−P = 2.239(1) Å for the Mo complex). The latter anionic complexes are protonated by $HBF_4 \cdot OEt_2$ to give the hydroxyphosphide derivatives $[MCp\{P(OH)R^*\}(CO)_2]$. In the presence of excess acid, the molybdenum complex yields the fluorophosphide complex $[MoCp(PFR^*)(CO)_2]$ (Mo−P = 2.204(1) Å), while the tungsten compound reacts with excess HCl to give an unstable chlorophosphine complex $[WCpCl(PHClR^*)(CO)_2]$ which is rapidly hydrolyzed to give $[WCpCl\{PH(OH)R^*\}(CO)_2]$, having a complexed arylphosphinous acid (Mo−P = 2.460(2) Å). The molybdenum anion reacts with strong C-based electrophiles such as $[Me_3O]BF_4$, Et_2SO_4, $C_2H_3C(O)Cl$, and PhC(O)Cl to give the corresponding alkoxyphosphide derivatives $[MoCp\{P(OR)R^*\}(CO)_2]$ (R = Me, Et, COC_2H_3, COPh; Mo−P = 2.197(2) Å for the benzoyl compound), as a result of the attack of the electrophile at the O atom of the oxophosphinidene ligand. In contrast, the reactions with milder alkylating reagents such as the alkyl halides MeI, EtI, C_3H_5Br, and C_3H_3Br give selectively the corresponding κ^2-phosphinite complexes $[MoCp\{\kappa^2\text{-}OP(R)R^*\}(CO)_2]$ [R = Me, Et, C_3H_5, C_3H_3; Mo−P = 2.3733(5) Å for the allyl compound] as a result of the attack of the electrophile at the P atom of the oxophosphinidene ligand. According to density functional theory (DFT) calculations, the oxygen atom of the phosphinidene ligand bears the highest negative charge in the molybdenum anion, while the highest occupied molecular orbital (HOMO) of this complex has substantial Mo−P π bonding character. Thus, it is concluded that the phosphinite complexes are formed under conditions of orbital control, while charge-controlled reactions tend to give alkoxyphosphide derivatives.

Introduction

A challenge for chemists in the process of understanding the paths connecting the reactants to the final products in a particular reaction is the identification or proposal of intermediate species which are often very unstable or just undetectable molecules. Within the chemistry of organophosphorus compounds, one such class of substances that have been proposed as intermediates in different reactions, often with little or no mechanistic data, are phosphinidene oxides (R−P═O). In contrast to their nitrogen analogues RNO, which are isolable and commercially available species, phosphinidene oxides are unstable molecules in ordinary conditions but are thought to be generated in the thermal or photochemical decomposition of several precursors such as phospholene, phosphirane, or phosphanorbornadiene oxides, and others.[1] These transient species undergo processes such as addition to dienes and diones, or insertion into O−H and S−S bonds, and are therefore interesting synthons for new organophosphorus derivatives.[1a,2]

Because of the similarity in the electronegativities of carbon and phosphorus, the bonding properties and chemical behavior of low-coordinated organophosphorus compounds can be similar to those of their carbon analogues. In particular, phosphinidene oxides can be isolobal-related to carbenes.[3] As it is the case of carbenes, stabilization of the reactive R−P═O species can be in principle achieved through coordination to metal centers, a strategy that could allow for a more detailed study of the chemical behavior of these unsaturated molecules. So far, however, only a few oxophosphinidene complexes have been reported and, although

*To whom correspondence should be addressed. E-mail: mara@uniovi.es (M.A.R.).

(1) (a) Gaspar, P. P.; Qian, H.; Beatty, A. M.; d'Avignon, D. A.; Kao, J. L.-F.; Watt, J. C.; Rath, N. P. *Tetrahedron* **2000**, *56*, 105. (b) Cowley, A. H.; Gabbaï, F. P.; Corbelin, S.; Decken, A. *Inorg. Chem.* **1995**, *34*, 5931. (c) Wang, K.; Emge, T. J.; Goldman, A. S. *Organometallics* **1994**, *13*, 2135.

(2) (a) Stille, J. K.; Eichelberger, J. L.; Higgins, J.; Freeburger, M. E. *J. Am. Chem. Soc.* **1972**, *94*, 4761. (b) Nakayama, S.; Yoshifuju, M.; Okazaki, R.; Inamoto, N. *Bull. Chem. Soc. Jpn.* **1975**, *48*, 546. (c) Quast, H.; Heuschmann, M. *Angew. Chem., Int. Ed. Engl.* **1978**, *17*, 867. (d) Quin, L. D.; Yao, E. U.; Szewczyk, J. *Tetrahedron Lett.* **1987**, *28*, 1077.

(3) Schoeller, W. W.; Niecke, E. *J. Chem. Soc., Chem. Commun.* **1982**, 569.

Published on Web 09/08/2010

Chart 1

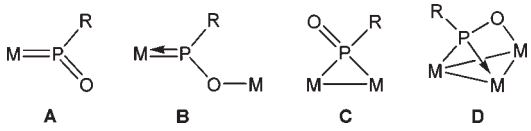

Chart 2

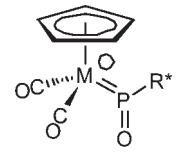

M = Mo (**3**), W (**3′**)

these display very different coordination modes of the RPO ligand, either terminal (**A**),[4a−c] μ_2-*P*,*O*-bridging (**B**),[4d] μ_2-*P*-bridging (**C**),[4e−g] or μ_3-*P*,*O*-bridging (**D**)[4g] ones (Chart 1), their reactivity has not been explored. Interestingly, we note that terminal oxophosphinidene complexes have been proposed as intermediates in the formation of dioxaphospholanes.[5]

Recently we reported the preparation of the $(H\text{-}DBU)^+$ salt of the anionic oxophosphinidene complex $[MoCp\{P(O)R^*\}(CO)_2]^-$ (**3**), (R* = 2,4,6-$C_6H_2{}^tBu_3$; Cp = η^5-C_5H_5, DBU = 1,8-diazabicyclo [5.4.0] undec-7-ene) from the hydride precursor $[Mo_2Cp_2(\mu\text{-}H)(\mu\text{-}PHR^*)(CO)_4]$ (**1**) via oxidation of the corresponding phosphide-bridged anion $(H\text{-}DBU)[Mo_2Cp_2(\mu\text{-}PHR^*)(CO)_4]$ (**2**).[6a] Preliminary studies of the reactivity of **3** toward different electrophiles and oxidizing reagents revealed that this complex, incidentally the first anionic oxophosphinidene complex reported in the literature, exhibited unique acid−base and redox properties with a multisite reactivity located at their O, P, and Mo atoms, depending on the reagent used.[6] In this paper we give full details of the preparation of **3** and that of its tungsten analogue $[WCp\{P(O)R^*\}(CO)_2]^-$ (**3′**) (Chart 2), and we analyze their reactions with several protic acids, and those of the molybdenum anion with a wide set of C-based electrophiles. As it will be discussed, the latter reactions allow for the synthesis of new alkoxyphosphide or *O*,*P*-phosphinite complexes, depending on the site of the attack of the electrophile to the coordinated oxophosphinidene ligand, a circumstance found in turn to be strongly dependent on the nature of the electrophilic reagent used. These experimental studies have been complemented with Density Functional Theory (DFT) calculations on the molybdenum anion **3**, for a better understanding of the structure and reactivity of these novel oxophosphinidene complexes.

Chart 3

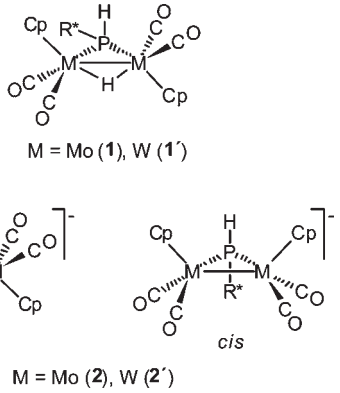

M = Mo (**2**), W (**2′**)

Results and Discussion

Preparation and Structure of the Anionic Complexes 3 and 3′. These mononuclear anions can be conveniently prepared following a two-step procedure. In the first step, the hydride-bridged complexes $[M_2Cp_2(\mu\text{-}H)(\mu\text{-}PHR^*)(CO)_4]$ [M = Mo (**1**), W (**1′**)] are easily and quantitatively deprotonated in tetrahydrofuran (THF) or dichloromethane solutions by a strong and non-coordinating base as DBU to give the corresponding salts $(H\text{-}DBU)[M_2Cp_2(\mu\text{-}PHR^*)(CO)_4]$ (M = Mo (**2**), W (**2′**), Chart 3), as revealed by IR and ^{31}P NMR spectroscopy. The tungsten complex **1′** had not been previously reported, but it can be prepared in yields above 50% by following the procedure previously described for the molybdenum compound **1**.[7] The IR spectrum of **1′** (Table 1) exhibits C−O stretching bands with a pattern comparable to those of related complexes of the type $[M_2Cp_2(\mu\text{-}H)(\mu\text{-}PRR')(CO)_4]$ (M = Mo, W), previously reported by us and others, and consistent with the more usual *transoid* arrangement of the $MCp(CO)_2$ fragments with respect to the average $M_2(\mu\text{-}H)(\mu\text{-}P)$ plane (Chart 3).[7] The ^1H and ^{13}C NMR spectra of **1′** are also consistent with the proposed structure and deserves no further comments.

As for the structure of the anions **2** and **2′**, previous work on related complexes reveals that the most common structure is that displaying a transoid arrangement of the $MCp(CO)_2$ fragments (Chart 3), as found in the hydride precursors and confirmed crystallographically in the case of the dimolybdenum complexes $[Mo_2Cp_2(\mu\text{-}PR_2)(CO)_4]^-$ (R = Ph,[8a] Me).[8b] However, the ^{31}P NMR spectra of the anions **2** and **2′** exhibit in each case a broad resonance at room temperature, while at the same time the IR spectrum exhibits more C−O stretching bands than expected for a single isomer. We have found previously these spectroscopic features in the alkoxyphosphide-bridged anions $[Mo_2Cp_2\{\mu\text{-}PCy(OR)\}(CO)_4]^-$ (R = CH_3, C_4H_5),[9] which we attributed to the presence in solution of both *cis* and *trans* isomers (Chart 3). In agreement with this, the NMR spectra of the tungsten compound **2′** is temperature-dependent, and at

(4) (a) Niecke, E.; Engelmann, M.; Zorn, H.; Krebs, B.; Henkel, G. *Angew. Chem., Int. Ed. Engl.* **1980**, *19*, 710. (b) Hitchcock, P. B.; Johnson, J. A.; Lemos, M. A. N. D. A.; Meidine, M. F.; Nixon, J. F.; Pombeiro, A. J. L. *J. Chem. Soc., Chem. Commun.* **1992**, 645. (c) Alvarez, M. A.; García, M. E.; González, R.; Ramos, A.; Ruiz, M. A. *Organometallics* **2010**, *29*, 1875. (d) Johnson, M. J. A.; Odom, A. L.; Cummins, C. C. *J. Chem. Soc., Chem. Commun.* **1997**, 1523. (e) Kourkine, V.; Glueck, D. S. *Inorg. Chem.* **1997**, *36*, 5160. (f) Schmitt, G.; Ullrich, D.; Wolmershäuser, G.; Regitz, M.; Scherer, O. J. *Z. Anorg. Allg. Chem.* **1999**, *625*, 702. (g) Alvarez, C. M.; Alvarez, M. A.; García, M. E.; González, R.; Ruiz, M. A. *Organometallics* **2005**, *24*, 5503. (h) Buchholz, D.; Huttner, G.; Imhof, W. *J. Organomet. Chem.* **1990**, *388*, 307.

(5) Marinetti, A.; Mathey, F. *Organometallics* **1987**, *6*, 2189.

(6) (a) Alonso, M.; García, M. E.; Ruiz, M. A.; Hamidov, H.; Jeffery, J. C. *J. Am. Chem. Soc.* **2004**, *126*, 13610. (b) Alonso, M.; Alvarez, M. A.; García, M. E.; Ruiz, M. A.; Hamidov, H.; Jeffery, J. C. *J. Am. Chem. Soc.* **2005**, *127*, 15012.

(7) Alvarez, C. M.; Alvarez, M. A.; García-Vivó, D.; García, M. E.; Ruiz, M. A.; Sáez, D.; Falvello, L. R.; Soler, T.; Herson, P. *Dalton Trans.* **2004**, 4168.

(8) (a) Hartung, H.; Walther, B.; Baumeister, U.; Böttcher, H. C.; Krug, A.; Rosche, F.; Jones, P. G. *Polyhedron* **1992**, *11*, 1563. (b) Petersen, J. L.; Stewart, R. P., Jr. *Inorg. Chem.* **1980**, *19*, 186.

(9) Alvarez, C. M.; Alvarez, M. A.; Alonso, M.; García, M. E.; Rueda, M. T.; Ruiz, M. A. *Inorg. Chem.* **2006**, *45*, 9593.

Table 1. IR and $^{31}P\{^1H\}$ NMR Data for New Compounds

compound	ν(CO)[a]/cm^{-1}	δ_P/ppm[b] [J_{PW}] /Hz
$[W_2Cp_2(\mu\text{-H})(\mu\text{-PHR*})(CO)_4]$ (**1′**)	1951 (w), 1931 (vs), 1853 (s)	3.0 [193][c]
(H-DBU)$[Mo_2Cp_2(\mu\text{-PHR*})(CO)_4]$ (**2**)	1891 (m), 1877 (m), 1844 (vs), 1826 (w, sh), 1769 (m)	130.3[d]
(H-DBU)$[W_2Cp_2(\mu\text{-PHR*})(CO)_4]$ (**2′**)	1883(m), 1870 (m), 1838 (vs), 1818 (w, sh), 1757 (m)	63.8 [252][e] (*cis*) 39.4 [277][e] (*trans*)
(H-DBU)[MoCp{P(O)R*}$(CO)_2$] (**3**)	1874 (vs), 1790 (s)[f], 1649 (m)[g]	385.0[h]
(H-DBU)[WCp{P(O)R*}$(CO)_2$] (**3′**)	1868 (vs), 1784 (s)	335.6 [658]
[MoCp{P(OH)R*}$(CO)_2$] (**4**)	1938 (vs), 1858 (s)	336.6[h]
[WCp{P(OH)R*}$(CO)_2$] (**4′**)	1928(vs), 1847 (s)	286.9 [704]
[MoCp(PFR*)$(CO)_2$] (**5**)	1959(vs), 1884 (s)	323.8[i]
[WCpCl(PHClR*)$(CO)_2$] (**6**)	1961(vs), 1876(s)	81.9 [308][j]
[WCpCl{PH(OH)R*}$(CO)_2$] (**7**)	1963(vs), 1881(s)	35.8 [286][k]
[MoCp{P(OMe)R*}$(CO)_2$] (**8a**)	1935(vs), 1856(s)	350.5
[MoCp{P(OEt)R*}$(CO)_2$] (**8b**)	1933(vs), 1853(s)	348.2
[MoCp{P(OC(O)C_2H_3)R*}$(CO)_2$] (**8c**)	1961 (vs), 1881 (s), 1725 (w)	291.5[h]
[MoCp{P(OC(O)Ph)R*}$(CO)_2$] (**8d**)	1961 (vs), 1882 (s), 1727 (w)	290.6
[MoCp(κ^2-OPMeR*)$(CO)_2$] (**9a**)	1940 (vs), 1850 (s)	28.3
[MoCp(κ^2-OPEtR*)$(CO)_2$] (**9b**)	1941 (vs), 1848 (s)	36.9
[MoCp{κ^2-OP(C_3H_5)R*}$(CO)_2$] (**9e**)	1942 (vs), 1852 (s)	33.5
[MoCp{κ^2-OP(C_3H_3)R*}$(CO)_2$] (**9f**)	1948 (vs), 1858 (s)	31.6

[a] C−O stretching frequencies recorded in dichloromethane solution, unless otherwise stated. [b] Recorded in CD_2Cl_2 solution at 290 K and 121.50 MHz unless otherwise stated; δ relative to external 85% aqueous H_3PO_4. [c] Recorded in $CDCl_3$ solution. [d] Recorded in THF solution at 290 K and 121.50 MHz. [e] Recorded in CD_2Cl_2 solution at 203 K and 162.14 MHz. [f] Recorded in THF. [g] C−N stretching band, recorded in Nujol mull. [h] 81.04 MHz. [i] J_{PF} = 1132 Hz. [j] J_{PH} = 422 Hz. [k] J_{PH} = 396 Hz.

203 K displays two separate ^{31}P resonances at 63.8 and 39.4 ppm, with 3:1 relative intensities, which we assign respectively to the *trans* and *cis* isomers on the basis of the analogy with the mentioned alkoxyphosphide-bridged complexes. At that temperature, independent ^1H NMR resonances are also observed for the cyclopentadienyl groups of **2′**, two at 5.36 and 5.13 ppm for the *trans* isomer and a single resonance at 5.26 ppm for the *cis* isomer. Although we have not studied in detail this isomerism for the dimolybdenum anion **2**, we note that its IR spectrum is very similar to that of the ditungsten anion **2′** (Table 1), and strongly reminiscent of those of the mentioned alkoxyphosphide-bridged anions.[9] Therefore, we conclude that *cis* and *trans* isomers are also present in the solutions of the dimolybdenum anion **2**.

The second step in the preparation of the mononuclear complexes **3** and **3′** involves the reaction of elemental oxygen with the anions **2** and **2′**, respectively. Although the formation of these mononuclear complexes from their binuclear precursors obviously requires the loss of a $MCp(CO)_2$ fragment and of a H atom at some stage, the inspection of the corresponding reaction mixtures by IR and ^{31}P NMR spectroscopy revealed the absence of any carbonyl- or phosphorus-containing species other than the mononuclear anions. Actually, the latter can be isolated in good yields from these solutions (ca. 60% after crystallization). Attempts to generate these products more efficiently by the reactions of the anions **2** and **2′** with other sources of oxygen atoms (H_2O_2, olefin oxides, amine oxides, etc.) were unsuccessful.

The structure or the molybdenum salt (H-DBU)[MoCp{P(O)R*}$(CO)_2$] (**3**) was determined through an X-ray diffraction study (Figure 1 and Table 2).[6a] The anion displays a terminally bound P(O)R* ligand (type **A** in Chart 1). Structurally characterized complexes of this type are restricted to the mononuclear complexes $[Cr(CO)_5\{P(O)N^iPr_2\}]$[4a] and $[ReCl(dppe)_2\{P(O)CH_2{}^tBu\}]$,[4b] and to the diiron complex $[Fe_2Cp_2(\mu\text{-CO})(CO)_2\{P(O)R^*\}]$, recently prepared in our laboratory.[4c] In all these species the phosphinidene ligand behaves as a two-electron donor, and

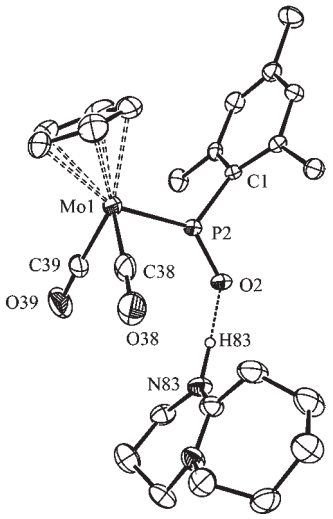

Figure 1. ORTEP diagram (30% probability) of the molecular structure of the anion and cation in compound **3**, with H atoms (except H83) and Me groups omitted for clarity.

Table 2. Selected Bond Lengths (Å) and Angles (deg) for Compounds **3**, **5**, and **8d**.[a]

parameter	**3**	**5**	**8d**
Mo−P	2.239(1)	2.204(1)	2.197 (2)
P−X	1.514(3)	1.614(2)	1.661(4)
P−C1	1.857(3)	1.829(4)	1.824(6)
C1−P−X	107.6(1)	97.3(2)	101.0(2)
Mo−P−X	132.7(1)	121.6(1)	135.6(2)
Mo−P−C1	119.7(1)	141.0(1)	123.2(2)
C2−Mo−C3	81.7(2)	84.4(2)	83.2(3)

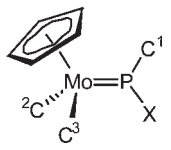

[a] Bond lengths and angles according to the labeling shown in the figure; X = O (**3**, **8d**), F (**5**); data taken from reference 6a.

the same applies to complex **3**. Noticeably the Mo−P length of 2.238(1) Å in **3** is substantially shorter than the values of

about 2.45 Å characteristic of single Mo→P donor bonds (e.g., Mo-PR_3 complexes) and much closer to the Mo−P lengths measured in molybdenum complexes having 3-electron P-donor ligands such as [Mo{$P(C_6H_{11})_2$}$_4$] (2.265(2) Å)[10] and [Mo(N^tBuAr)$_3${P(O*M*)(Me)}] (2.169(2) Å; *M* = $ZrCp_2Me$; Ar = 3,5-$Me_2C_6H_3$][4d] and several phosphide derivatives of **3** to be discussed later on (ca. 2.20 Å, Table 2). All of this suggests substantial double-bond character in the Mo−P bond of the oxophosphinidene ligand in **3**, a matter to be addressed later on in the light of DFT calculations. At the same time, the P−O length in **3** is also quite short (1.514(3) Å) and consistent with the formulation of a double bond, it being comparable to the values of about 1.49 Å measured in the three complexes of type **A** previously characterized,[4a−c] and even to that measured in the PO complex [Mo(N^tBuAr)$_3$(PO)] (1.49(2) Å).[4d] In agreement with this multiplicity of the Mo−P and P−O bonds, the coordination environment around phosphorus is planar trigonal (X−P−Y angles adding 360.0°). Moreover the Mo, P, O2 and C1 atoms are contained in a plane almost bisecting the anion (deviation ca. 6° from the ideal bisecting plane), with the aryl group oriented perpendicularly to it, thus excluding any π interaction of the aromatic ring with the oxophosphinidene ligand. As it will be discussed later on, this conformation maximizes the π interactions between the frontier orbitals of the Mo and P fragments. We also note that the aryl group is placed specifically *cis* to the Cp ligand of the complex. This conformation around the multiple Mo−P bond is also reproduced in all derivatives of **3** as discussed below, and it seems to be the one minimizing the steric repulsions originated from the bulky supermesityl group.

Nor unexpectedly, the anion and cation in the crystal lattice of **3** are not independent from each other, but linked through a hydrogen bond connecting the oxygen atom of the P(O)R* ligand and the N−H group of the $(H\text{-}DBU)^+$ cation (Figure 1). The corresponding separation N(H)···O is 2.673 Å (H···O = 1.524 Å), which is significantly shorter than the more common values of about 2.90 Å for N(H)···O hydrogen bonds,[11] thus indicating a quite strong interaction in our case.

Spectroscopic data in solution for **3** and **3′** are similar to each other (Table 1) and consistent with the solid-state structure of the molybdenum anion, and otherwise might be related to the structure of the neutral chlorophosphide complexes [MCp(PClR*)$(CO)_2$] [M = Mo, W].[12] The anionic nature of complexes **3** and **3′**, however, causes a significant reduction in the two C−O stretching frequencies of the carbonyl groups, as expected. On the other hand, both complexes exhibit strongly deshielded ^{31}P NMR resonances, with the tungsten complex displaying a large P−W coupling of 658 Hz. This almost doubles the values commonly observed for single W−P bonds in comparable complexes having PR_3 or PR_2-bridged ligands (ca. 200−400 Hz) and is thus taken as an independent indicator of the multiple nature of the M−P bonds in these oxophosphinidene complexes. All other spectroscopic features of the ^1H and ^{13}C NMR spectra are consistent with the retention of a symmetry plane bisecting the anions in solution and deserve no further comments. We note, however, the strong deshielding of the N−H protons in solution (δ = 13.88 ppm (**3**) and 12.43 ppm (**3′**), in dichloromethane solution), indicative of the persistence of significant hydrogen bonding in solution, as also suggested by the good solubility of these salts in nonpolar solvents such as toluene and diethylether.

Chart 4

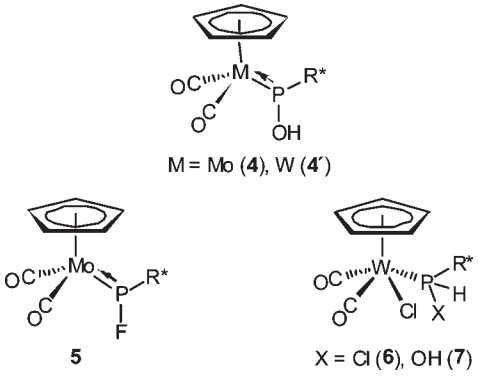

Protonation Reactions of Compounds 3 and 3′. These anionic complexes are readily and reversibly protonated at the oxygen atom of the oxophosphinidene ligand with different weak protic acids such as $(NH_4)PF_6$ and $B(OH)_3$, or with stoichiometric amounts of the strong acids HCl (3.2 M in Et_2O) and $HBF_4\cdot Et_2O$ (54% in Et_2O), to give the corresponding hydroxyphosphide complexes [MCp{P(OH)-R*}$(CO)_2$] quantitatively (M = Mo (**4**), W (**4′**), Chart 4). In the case of the strong acids, however, a different and irreversible result is obtained if using two or more equiv of acid. Thus, the molybdenum compound **3** reacts with 2 equiv of $HBF_4\cdot Et_2O$ (54%) to give the fluorophosphide complex [MoCp(PFR*)$(CO)_2$] (**5**) quantitatively, but a more complex mixture of products was obtained when using excess HCl, which we could not fully characterize (see below). The tungsten anion **3′** reacted in the opposite way: when using excess HBF_4 then a mixture of complexes was obtained which we could neither characterize properly, but the reaction with excess HCl turned out to be more selective. A monitoring of the latter reaction in dichloromethane solution at room temperature (using IR and ^{31}P NMR spectroscopy) revealed that the hydroxyphosphide complex **4′** was the species first formed, this being rapidly transformed into a second species tentatively identified as the chlorocomplex [WClCp{PH-(Cl)R*}$(CO)_2$] (**6**), having a chlorophosphine ligand coordinated to tungsten. The latter complex, however, could not be isolated as a pure material since it readily hydrolyzes upon manipulation (rapidly upon addition of water to the reaction mixture) to cleanly give the chlorocomplex [WClCp{PH-(OH)R*}$(CO)_2$] (**7**), having a coordinated molecule of the phosphinous acid PH(OH)R*, which is the species finally isolated. Since there are two asymmetric centers in this molecule (the metal center and the phosphorus atom), then two diastereoisomers might be obtained. However, only a single isomer is obtained in this reaction, possibly favored by the presence of intramolecular hydrogen bonding in it (see later).

As noted above, the reaction of the molybdenum anion **3** with excess HCl gave a mixture of products. The two

(10) Baker, R. T.; Krusic, P. J.; Tulip, T. H.; Calabrese, J. C.; Wreford, S. S. *J. Am. Chem. Soc.* **1983**, *105*, 6763.
(11) Huheey, J. E.; Keiter, E. A.; Keiter, R. L. *Inorganic Chemistry: Principles of Structure and Reactivity*, 4th ed.; HarperCollins College Publishers: New York, 1993; p 301.
(12) Malisch, W.; Hirth, U.-A.; Grün, K.; Schmeuber, M. *J. Organomet. Chem.* **1999**, *572*, 207.

Scheme 1. Ligand Transformations in the Protonation Reactions of the Anions **3** and **3′**

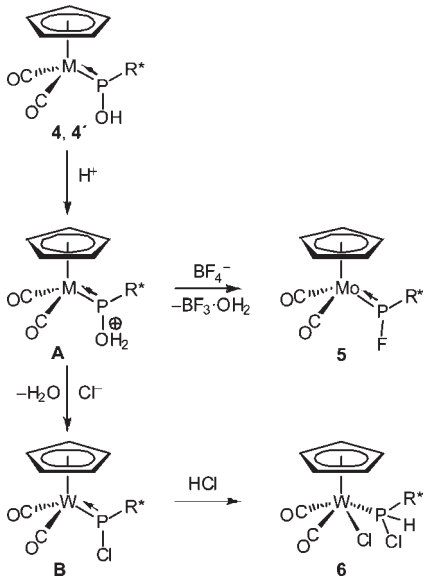

major species present in that mixture have spectroscopic properties comparable respectively to those of the tungsten product **6** (δ_P = 110.6 ppm, J_{PH} = 413 Hz) and to those of **7** (δ_P = 69.2 ppm, J_{PH} = 386 Hz), if we take into account the expected modifications operated on the ^{31}P chemical shifts when replacing W with Mo. Unfortunately we could isolate neither of them as pure materials.

The formation of compounds **5** to **7** implies the unusual transformation of P−OH bonds into P−halogen bonds, and it can be understood by assuming that in the presence of a second equivalent of a strong acid then the protonation of the hydroxyl group in compounds **4** and **4′** would occur to some extent thus favoring the replacement of an H_2O molecule by a halide anion coming from the added acid (Scheme 1). In the reaction with HBF_4, this might be additionally facilitated by the formation of the $BF_3 \cdot OH_2$ adduct and leads directly to the fluorophosphide complex **5** (Scheme 1). In the reaction with HCl, such a process would initially give a related chlorophosphide complex **B** (not detected) which would then add another HCl molecule to its double Mo−P bond, in a regiospecific way, to give the chlorocomplex **6**, which then can undergo easily a classical hydrolytic process to give **7**.

Reactions of Compound 3 with C-based Electrophiles. The title reactions have been found to be strongly dependent on the electrophilic reagent used. They can involve either the formation of a new C−O bond between the hydrocarbon fragment and the oxygen atom of the oxophosphinidene ligand, to give an alkoxyphosphide derivative, or the formation of a new C−P bond with the phosphorus atom of the oxophosphinidene ligand, to give a *P,O*-bound phosphinite complex (Scheme 2). These reactions seem to be highly regioselective, since in most cases we observe the formation of just one of the two types of products when using a single reagent.

The formation of a new C−O bond is the dominant process when using strong electrophilic reagents such a $[Me_3O][BF_4]$, Et_2SO_4, and acid chlorides. Thus compound **3** reacts instantaneously at room temperature with $[Me_3O][BF_4]$ to give the methoxyphosphide complex

Scheme 2. Reactions of the Anion **3** with C-based Electrophiles. [(i) $(Me_3O)BF_4$, Et_2SO_4, $C_2H_3C(O)Cl$ or $PhC(O)Cl$; (ii) MeI, EtI, C_3H_5Br or C_3H_3Br]

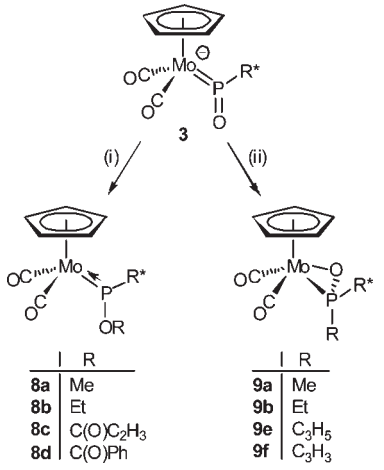

$[MoCp\{P(OMe)R^*\}(CO)_2]$ (**8a**), and a similar reaction takes place with Et_2SO_4 to give the ethoxyphosphide complex $[MoCp\{P(OEt)R^*\}(CO)_2]$ (**8b**), although the reaction is now expectedly slower and requires about 2 h for completion. The same result is obtained with acryloyl chloride, which gives the corresponding alkoxyphosphide derivative $[MoCp\{P(OC(O)C_2H_3)R^*\}(CO)_2]$ (**8c**) in about 15 min at room temperature. In contrast, compound **3** and benzoyl chloride react in dichloromethane solution to reach an equilibrium with the corresponding alkoxyphosphide derivative $[MoCp\{P(OC(O)Ph)R^*\}(CO)_2]$ (**8d**). The IR spectra of the reaction mixture reveal the presence of the characteristic C−O stretching bands of both complexes **3** and **8d**, with those of the neutral product increasing their relative intensity upon increasing the excess of reagent being added. At the same time, the ^{31}P NMR spectra of these reaction mixtures display just a single and broad resonance at a chemical shift intermediate between those corresponding to **3** and **8d**, (385.0 and 290.6 ppm, respectively), thus indicating that the forward and back reactions connecting the anion and the neutral derivative are fast enough on the NMR time scale. Clearly the corresponding equilibrium is facilitated by the solubility of the salt (H-DBU)Cl in dichloromethane. In agreement with this interpretation, upon removal of the solvent and addition of a low-polarity solvent as petroleum ether to the residue, a solution containing exclusively the neutral product **8d** is obtained, thus allowing the isolation of this complex in the conventional way.

In contrast, the formation of a new C−P bond is the dominant process when using milder electrophilic reagents such as alkyl halides. Thus the reactions with methyl or ethyl iodide, allyl bromide, or propargyl bromide proceed smoothly at room temperature or 303 K (EtI) to give the corresponding phosphinite derivatives $[MoCp(\kappa^2\text{-}OPRR^*)(CO)_2]$ (R = Me (**9a**), Et (**9b**), C_3H_5 (**9e**), C_3H_3 (**9f**)), which are isolated as cherry-red solids in high yields (Scheme 2). It is to be noted that the nature of the halide has a measurable influence not only on the rate but also on the product distribution in these reactions. For instance, if allyl chloride is used instead of the bromide, then the reaction proceeds at a slower rate but, more interestingly, a small amount of a minor species, tentatively identified as the corresponding alkoxyphosphide complex $[MoCp\{P(OCH_2CHCH_2)R^*\}(CO)_2]$, is

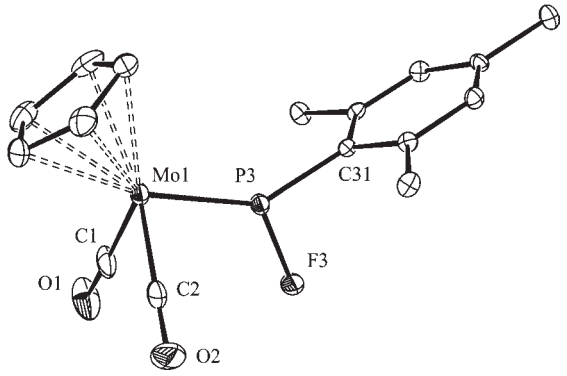

Figure 2. ORTEP diagram (30% probability) of the molecular structure of compound **5**, with H atoms and Me groups omitted for clarity.

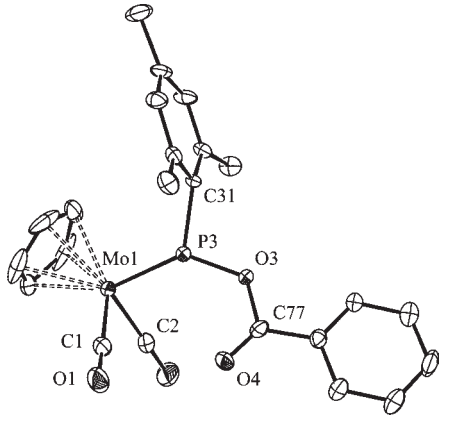

Figure 3. ORTEP diagram (30% probability) of the molecular structure of compound **8d**, with H atoms and Me groups omitted for clarity.

detected in the ^{31}P NMR spectrum of the crude reaction mixture. This side product is only present as trace amounts if using allyl bromide. The effect on the reaction rate can be explained on the basis of the higher strength of the C−X bond to be broken (D(C−Cl) > D(C−Br)).[13] On the other hand, the appearance of small amounts of the alkoxyphosphide complex indicates that, for a fixed hydrocarbon fragment, the attack of the electrophilic reagent at the O atom of the oxophosphinidene ligand is facilitated upon increasing the positive charge at the carbon atom, as also indicated by the completely different outcome of the reactions with $[Me_3O]BF_4$ and MeI. This matter will be further addressed later in the light of the DFT calculations performed on **3**.

Structural Characterization of Compounds 4, 5, and 8. The structures of the fluorophosphide complex **5** and the alkoxyphosphide complex **8d** were confirmed through single crystal X-ray diffraction studies,[6a] and are shown in the Figures 2 and 3, while the relevant bond lengths and angles are assembled in the Table 2 for comparative purposes. Both molecules display a phosphide ligand bound to a $MoCp(CO)_2$ with a trigonal environment around phosphorus (sum of X−P−Y angles ca. 360°), although the individual values of the X−P−Y angles depart from the ideal figure of 120° as required to minimize the steric repulsions. The conformation of the phosphide ligand is identical to that of the oxophosphinidene ligand in the anion **3**, that is, with the ligand plane bisecting the $MoCp(CO)_2$ fragment and the supermesityl group arranged close to the Cp ligand. As noted above, this conformation maximizes the π interaction between the frontier orbitals of the Mo and P fragments and now allows the phosphide ligand to act as a three-electron donor group. In agreement with this, the Mo−P lengths of 2.204(1) Å (**5**) and 2.197(2) Å (**8d**) are consistent with the formulation of double bonds, and are in fact marginally shorter than the corresponding lengths measured in related chloro-, amino-, and alkoxyphosphide complexes such as $[MoCp\{PCl(tmp)\}(CO)_2]$ (tmp = tetramethylpiperidyl, Mo−P = 2.214(2) Å),[14] $[MoCp\{P(NMe_2)(tmp)\}(CO)_2]$ (2.243(2) Å),[14] and $[MoCp\{PCH(SiMe_3)_2(OEt)\}(CO)_2]$ (2.207(2) Å),[15] and also slightly shorter than that in the starting anion **3**. In contrast, the P−O length in **8d** (1.661(4) Å) is now much longer than that in **3** (1.514(3) Å), as expected from the reduction operated in the corresponding bond order (from two to one) upon alkylation at the O atom of the oxophosphinidene ligand.

Spectroscopic data in solution for compounds **4**, **4′**, **5**, and **8a**−**d** are comparable to each other and consistent with the structures found for **5** and **8d** in the crystal. Moreover, the data are also similar to those reported for comparable phosphide complexes having a supermesityl substituent, such as $[MCp(PHR^*)(CO)_2]$ and $[MCp(PClR^*)(CO)_2]$ (M = Mo, W).[12] We first note the expected ordering of the C−O stretching frequencies in the molybdenum complexes as both the electronegativity and the acceptor properties of the substituent at phosphorus increase, yielding an ordering OEt < OMe < OH ≪ F < C(O)R. On the other hand, these compounds give rise to quite deshielded ^{31}P resonances, in the range 290−350 ppm. The latter can be explained by the combination of two effects of known deshielding influence on P-donor ligands, the presence of a very electronegative atom (O or F) bound to phosphorus, and the multiple nature of the metal−phosphorus bond.[16] This also justifies the fact that our complexes display ^{31}P shifts substantially higher than those of the mentioned complexes $[MoCp(PXR^*)(CO)_2]$ (X = H (266.2 ppm), Cl (259.1 ppm)).[12] As it can be inferred also from the values in the Table 1, there is a roughly reverse correlation between the C−O stretching frequencies and the ^{31}P chemical shifts, so that the electron poorer metal centers are associated with the lower ^{31}P shifts. This suggests that the paramagnetic contribution to the shielding of the phosphorus atom might be dominant, once again in agreement with the multiple nature of the metal−phosphorus bond,[17] although the fine details of this influence are difficult to justify on a simple basis. The tungsten complex **4′** displays C−O stretching frequencies lower and ^{31}P NMR resonances more shielded than those of its molybdenum analogue **4**, as generally observed when comparing related W and Mo complexes. Moreover, the corresponding P−W coupling

(13) Huheey, J. E.; Keiter, E. A.; Keiter, R. L. *Inorganic Chemistry: Principles of Structure and Reactivity*, 4th ed.; HarperCollins College Publishers: New York, 1993; p A30.

(14) Cowley, A. H.; Giolando, D. N.; Nunn, C. M.; Pakulski, M.; Westmoreland, D.; Norman, N. C. *J. Chem. Soc., Dalton Trans.* **1988**, 2127.

(15) Arif, A. M.; Cowley, A. H.; Nunn, C. M.; Quashie, S. *Organometallics* **1989**, *8*, 1878.

(16) Carty, A. J.; MacLaughlin, S. A.; Nucciarone, D. In *Phosphorus-31 NMR Spectroscopy in Stereochemical Analysis*; Verkade, J. G., Quin, L. D., Eds.; VCH: Deerfield Beach, FL, 1987; Chapter 16.

(17) Jameson, C. J.; Mason, J. In *Multinuclear NMR*; Mason, J., Ed.; Plenum Press: New York, 1987; Chapter 3.

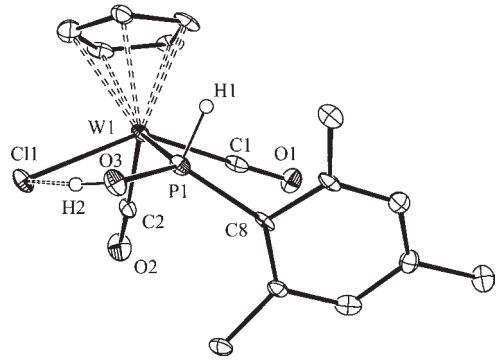

Figure 4. ORTEP diagram (30% probability) of the molecular structure of compound **7**, with H atoms (except H1 and H2) and Me groups omitted for clarity.

(704 Hz) is even higher than that in the starting anion **3′**, which is again consistent with a description of the W−P interaction as a double bond. For comparison, the W−P coupling in the complex [WCp(PClR*)(CO)$_2$] has a very similar value (711.6 Hz).[12] We finally note that the fluorophosphide complex **5** exhibits a very large P−F coupling (1132 Hz), some 200 Hz higher than the values measured previously for several fluorophosphide-bridged complexes [$Mo_2Cp_2(\mu$-H)(μ-PFR)(CO)$_4$],[7] which is another spectroscopic indicator of the trigonal environment around phosphorus, and the increased s orbital contribution from phosphorus to the P−F bond implied by that geometry. We note here that a more direct spectroscopic comparison is not possible, since apparently compound **5** is the first complex reported with a trigonal fluorophosphide (PFR) ligand. Other spectroscopic features of the NMR spectra of compounds **4**, **5**, and **8** are as expected and deserve no further comments.

Structural Characterization of Compounds 6 and 7. The structure of the chlorocomplex **7** in the crystal is shown in Figure 4, while the most relevant bond distances and angles are collected in Table 3. The molecule displays a classical four-legged piano stool geometry with a *cis* arrangement of the carbonyl ligands (C−W−C = 77.8(3)°), the other two coordination positions being occupied by a chloride ligand and a P−bound molecule of the supermesitylphosphinous acid, which is the unstable tautomer of the supermesitylphosphine oxide (P(O)H$_2$R*). The W−P length of 2.460(2) Å has a value typical of phosphine complexes in comparable Mo or W complexes, and is much longer than the double-bond lengths measured for compounds **3**, **5**, and **8d**, as expected. A noticeable structural feature in this molecule is the presence of significant intramolecular hydrogen bonding involving the chloride ligand and the hydroxyl group of the phosphorus ligand, as revealed by the short OH···Cl normalized distance[18] of 0.78 (H···Cl = 2.317 Å) and feasible orientation of the donor and the acceptor (Mo−Cl···H = 84.8°; Cl···H−O 148.5°).[19] This intramolecular interaction is comparable to that found by us previously in the related bromocomplex *cis*-[MoBrCp{P(CH$_2$CMe$_2$C$_6$H$_2$-^{t}Bu$_2$(OH)}(CO)$_2$] [normalized distance H···Br = 0.80, Mo−Br···H = 82.1°, Br···H−O = 145.4°].[6b] In contrast, the hydride complex [WHCp{PH(OH)^{t}Bu}(CO)$_2$] with a structure analogous to that of **7**, cannot be involved in similar intramolecular interactions, and actually arranges in the crystal in dimers held by OH···OC contacts between the hydroxyl substituent of one molecule and a carbonyl ligand of the adjacent one.[20a]

Table 3. Selected Bond Lengths (Å) and Angles (deg) for Compounds **7** and **9c**

7		**9c**[a]	
W(1)−P(1)	2.460(2)	Mo(1)−P(3)	2.3733(5)
P(1)−O(3)	1.590(7)	Mo(1)−O(3)	2.197 (1)
P(1)−H(1)	1.30(2)	P(3)−O(3)	1.555(1)
P(1)−C(8)	1.823(9)	P(3)−C(31)	1.841(2)
O(3)−H(2)	0.83(2)	P(3)−C(3)	1.853(2)
Cl(1)···H(1)	2.317	C(3)−C(4)	1.493(2)
Cl(1)···O(3)	3.049	C(4)−C(5)	1.317(3)
C(2)−W(1)−C(1)	77.8(3)	Mo(1)−C(1)	1.947(2)
P(1)−W(1)−Cl(1)	81.6(1)	Mo(1)−C(2)	1.959(2)
C(8)−P(1)−W(1)	122.4(3)	C(31)−P(3)−C(3)	115.1(1)
O(3)−P(1)−H(1)	94(3)	C(31)−P(3)−Mo(1)	119.6(1)
C(8)−P(1)−H(1)	94(3)	C(3)−P(3)−Mo(1)	123.7(1)
W(1)−P(1)−(O3)	117.1(3)	C(31)−P(3)−O(3)	110.9(1)
C(8)−P(1)−O(3)	111.6(4)	C(3)−P(3)−O(3)	107.8(1)
W(1)−P(1)−H(1)	111(3)	C(1)−Mo(1)−P(3)	86.9(1)
Cl(1)···H(1)−O(3)	148.5	C(1)−Mo(1)−C(2)	76.1(1)
		O(3)−Mo(1)−P(3)	39.5(1)
		C(2)−Mo(1)−O(3)	87.8(1)
		O(3)−P(3)−Mo(1)	64.1(1)

[a] Data taken from reference 6a.

Spectroscopic data in solution for **7** (Table 1 and Experimental Section) are consistent with the structure found in the crystal. In the first place, this complex exhibits two C−O stretching bands with relative intensities characteristic of the presence of a *cisoid* M(CO)$_2$ oscillator, and with positions comparable to those of the related phosphine complex [WCpCl(CO)$_2$(PH$_2$Mes)] (Mes = 2,4,6-C$_6$H$_2$Me$_3$).[20b] In contrast, the chemical shift of the ^{31}P nucleus in **7** (35.8 ppm) is much higher than those in the above complex (−78.9 ppm), or in [WCpCl(CO)$_2$(PH$_2$R*)] (−71.4 ppm),[12] because of the presence of the hydroxyl group bound to phosphorus. Yet, its chemical shift is still lower than that of the bound phosphinous acid in [WHCp{PH(OH)^{t}Bu}(CO)$_2$] (δ_P = 133.4 ppm, J_{PW} = 281 Hz),[20a] a difference that can attributed to the distinct hydrocarbon substituents at phosphorus, but the P−W couplings are very similar (286 Hz for **7**). These values are much lower than those in **3′** and **4′** (ca. 700 Hz) as a result of the reduction in the Mo−P bond order and the increase in the number of ligands around the tungsten atom.[21] The ^{1}H NMR spectrum of **7** displays inequivalent resonances for the ^{t}Bu groups, indicating the retention of a rigid structure in solution, and a P−H resonance with unremarkable parameters (δ_H = 9.22 ppm; J_{HP} = 396 Hz). The O−H resonance is not particularly deshielded (δ_H = 7.11 ppm; J_{HH} = 3 Hz), but the fact that it exhibits coupling with the P-bound hydrogen indicates a non dissociative behavior, possibly because of

(18) Brammer, L.; Bruton, E. A.; Sherwood, P. *Cryst. Growth Des.* **2001**, *1*, 277.
(19) Steiner, T. *Angew. Chem., Int. Ed.* **2002**, *41*, 48.
(20) (a) Malisch, W.; Hirth, U.-A.; Grün, K.; Schmeusser, M.; Fey, O.; Weis, U. *Angew. Chem., Int. Ed. Engl.* **1995**, *34*, 2500. (b) Malisch, W.; Hirth, U.-A.; Bright, T. A.; Käb, H.; Ertel, T. S.; Hückmann, S.; Bertagnolli, H. *Angew. Chem., Int. Ed. Engl.* **1992**, *31*, 1525.
(21) (a) Lambert, J. A.; Mazzola, E. P. *Nuclear Magnetic Resonance. An Introduction to Principles and Experimental Methods*; Pearson: London, 2003. (b) Jameson, C. J. In *Phosphorus-31 NMR Spectroscopy in Stereochemical Analysis*; Verkade, J. G., Quin, L. D., Eds.; VCH: Deerfield Beach, FL, 1987; Chapter 6.

the retention of significant O−H···Cl hydrogen bonding in solution.

The structure of the readily hydrolyzable complex **6**, proposed to be identical to that of **7** except for the presence of a P−Cl bond instead of a P−OH one in the phosphorus ligand, can be guessed by comparison of the spectroscopic data of these two compounds. Actually, the IR spectra of both complexes are quite similar, and the respective P−H and P−W couplings have comparable values (Table 1). The main effect of the presence of the electronegative chlorine atom bound to phosphorus (instead of the hydroxyl group) is a significant increase in the ^{31}P chemical shift (by ca. 45 ppm), and in the P−H and P−W couplings (by 26 and 22 Hz respectively) of the phosphorus ligand. The higher chemical shift of the chlorophosphine complex **6** (compared to that of **7**) follows the general trend observed for the free ligands.[17] As for the larger P−H and P−W couplings in **6** (422 and 308 Hz respectively), we first note that these figures are very similar to those reported for the strongly related chlorophenylphosphine complex $[WCp(CO)_2Cl(PClHPh)]$ (412 and 313 Hz, respectively).[22] Moreover, the latter couplings decrease to 408 and 308 Hz respectively in the corresponding amidophosphine complex $[WCp(CO)_2Cl\{P(N(SiMe_3)_2)HPh\}]$,[22] a change of the same sign as the one between **6** and **7**, but less pronounced. In spite of this, we must say that the fine details of the changes in one-bond coupling constants to phosphorus in this sort of compounds are difficult to be justified on a single parameter such as the electronegativity of the substituents at phosphorus.[21] For instance, replacing a chlorine atom by an amido group in the tungsten chlorophosphine complex $[W(CO)_5\{PHCl(CH(SiMe_3)_2)\}]$ causes a decrease in the value of J_{PW}, but an increase in the magnitude of the corresponding J_{PH}.[23]

Structural Characterization of Compounds 9. The structure of complex **9e** was determined through a single-crystal X-ray study and is shown in the Figure 5,[6a] while the relevant structural data are given in the Table 3. The most significant feature in this dicarbonyl complex is the presence of a *P*,*O*-bound phosphinite ligand originated from the attachment of the allyl group to the phosphorus atom of the oxophosphinidene ligand of **3**. As a result, the coordination geometry of the metal atom can be described as an expectedly distorted version of the conventional four-legged piano stool type. The environment around phosphorus, however, is rather unusual because, instead of displaying a tetrahedral environment, the P, Mo, C(3), and C(31) atoms are placed almost in the same plane (sum of X−P−Y angles 358.4°), while the oxygen atom is placed out of this plane, over the Mo−P bond, this implying a very acute Mo−P−O and P−Mo−O angles.This unnatural geometry is in part forced by the simultaneous coordination of the P and O atoms to phosphorus, and also in part derived from the steric repulsions operating between the supermesityl group and the $MoCo(CO)_2$ fragment. Interestingly, a similar environment around phosphorus has also been found for

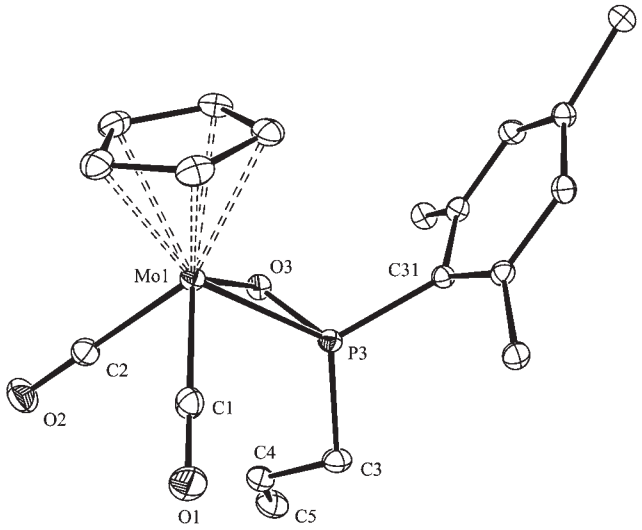

Figure 5. ORTEP diagram (30% probability) of the molecular structure of compound **9e**, with H atoms and Me groups omitted for clarity.

the isoelectronic thiophosphinite complexes $[WCp(\kappa^2\text{-}SPCl^tBu)(CO)_2]$,[24] $[WCp\{\kappa^2\text{-}SPMeN(SiMe_3)_2\}(CO)_2]$,[25] and $[Mo(C_6H_7)(\kappa^2\text{-}SPMe_2)(CO)_2]$.[26] We note that no other complexes containing *P*,*O*-bound phosphinite ligands appear to have been reported previously.

Spectroscopic data in solution for all four compounds **9a**−**f** are similar to each other and consistent with the structure found for **9e** in the crystal. They exhibit two C−O stretching bands in the IR spectrum with the characteristic pattern of *cis*-$M(CO)_2$ oscillators in a position comparable to their isomeric alkoxyphosphide complexes **8**. However, the simultaneous coordination of the P and O atoms of the phosphinite ligand in compounds **9** now makes the CO ligands inequivalent and, accordingly, these complexes exhibit two different carbonyl resonances in the ^{13}C NMR spectra, these appearing as a doublet (J_{CP} ca. 26 Hz) and as a singlet, as expected for carbonyl ligands respectively *cis* and *trans* to phosphorus ligands in four-legged piano stool complexes of the type $[MCpX(CO)_2(PR_3)]$ (M = Mo, W; X = H, halogen, R, etc.).[27] The phosphinite ligand in compounds **9** gives rise to strongly shielded resonances at around 30 ppm, that is, some 300 ppm lower than their tautomeric alkoxyphosphide complexes **8**. This dramatic shielding can be hardly attributed exclusively to the change operated in the coordination number of phosphorus (increase from 3 to 4),[28] but possibly is also related to the formation of a strained MoOP ring. The ^{1}H and ^{13}C NMR spectra of compounds **9** display the characteristic resonances of each hydrocarbon group bound to phosphorus and deserve no special comments. We note, however, that in all cases two different resonances are observed for

(22) Reisacher, H. U.; Duesler, E. N.; Paine, R. T. *J. Organomet. Chem.* **1998**, *564*, 13.
(23) Streubel, R.; Priemer, S.; Ruthe, F.; Jones, P. G. *Eur. J. Inorg. Chem.* **2000**, 1253.
(24) Malisch, W.; Grün, K.; Hirth, U.-A; Noltemeyer, M. *J. Organomet. Chem.* **1996**, *513*, 31.
(25) Reisacher, H.-U.; McNamara, W. F.; Duesler, E. N.; Paine, R. T. *Organometallics* **1997**, *16*, 449.
(26) Alper, H.; Einstein, F. W. B.; Harstock, F. W.; Jones, R. H. *Organometallics* **1987**, *6*, 829.
(27) (a) Todd, L. J.; Wilkinson, J. R.; Hickley, J. P.; Beach, D. L.; Barnett, K. W. *J. Organomet. Chem.* **1978**, *154*, 151. (b) Wrackmeyer, B.; Alt, H. G.; Maisel, H. E. *J. Organomet. Chem.* **1990**, *399*, 125.
(28) Fluck, E.; Heckmann, G. In *Phosphorus-31 NMR Spectroscopy in Stereochemical Analysis*; Verkade, J. G., Quin, L. D., Eds.; VCH: Deerfield Beach, FL, 1987; Chapter 2.

Table 4. Selected Bond Lengths (A) and Angles (deg) for the DFT-Optimized Geometry of the Anion $[MoCp\{P(O)R^*\}(CO)_2]^-$

parameter	calcd	exp (**3**)
Mo−P	2.287	2.239(1)
P−O	1.518	1.514(3)
Mo−C1	1.954	1.914(5)
Mo−C2	1.961	1.932(5)
C1−O1	1.168	1.177(5)
C2−O2	1.168	1.167(5)
P−C(aryl)	1.905	1.857(3)
Mo−P−O	136.0	132.7(1)
Mo−P−C(aryl)	115.6	119.7(1)
C1−Mo−C2	85.0	81.7(2)
C1−Mo−P−O	31.0	35.4
C2−Mo−P−O	−53.9	−46.3

the *ortho*-^{t}Bu groups, which indicates that there is enough crowding in these molecules to prevent their aryl groups from fast rotation in solution.

DFT Calculations on the Anion $[MoCp(CO)_2\{P(O)R^*\}]^-$. Analysis of Its Structure and Reactivity. As we have seen in the preceding sections, the reactions of the anionic complex **3** with different electrophilic reagents can result initially in the attachment of the incoming electrophile at the O site of the oxophosphinidene ligand (compounds **4** and **8**) or at its P site (compounds **9**). To better understand the origin of this regioselectivity we have carried out DFT[29] calculations on the molybdenum anion (see the Experimental Section for details). The electronic structure and bonding in this oxophosphinidene complex have been analyzed mainly through the properties of the relevant molecular orbitals, but the topological properties of the electron density, as managed in the Atoms in Molecules (AIM) theory,[30] have been also examined.

The most relevant parameters derived from the geometry optimization of the anion are collected in the Table 4, with the corresponding view being shown in the Figure 6. The optimized bond lengths are in quite good agreement with the corresponding experimental data of its $(H\text{-}DBU)^+$ salt discussed above, although the computed values for lengths involving the metal atom tend to be slightly longer (by less than 0.05 Å) than the corresponding experimental data. This is a common trend with the functionals currently used in the DFT computations of transition metal compounds.[29a,31] As expected, short Mo−P (2.287 Å) and P−O (1.518 Å) lengths are computed for this molecule, in agreement with the substantial double-bond character presumed for these bonds. Noticeably, the average plane defined by the Mo, P, O, and C(aryl) atoms of the oxophosphinidene ligand is slightly twisted (by ca. 12°) with respect to the plane bisecting the $MoCp(CO)_2$ fragment, a structural feature also present in the crystal structure of the $(H\text{-}DBU)^+$ salt (twisting by ca. 6°). As shown below, this would not be an accidental distortion, but one favoring several interactions, including a moderate hydrogen bonding with one of the H(Me) atoms of the *ortho*-^{t}Bu groups (O···H = 2.182 Å, normalized distance = 0.81), a feature

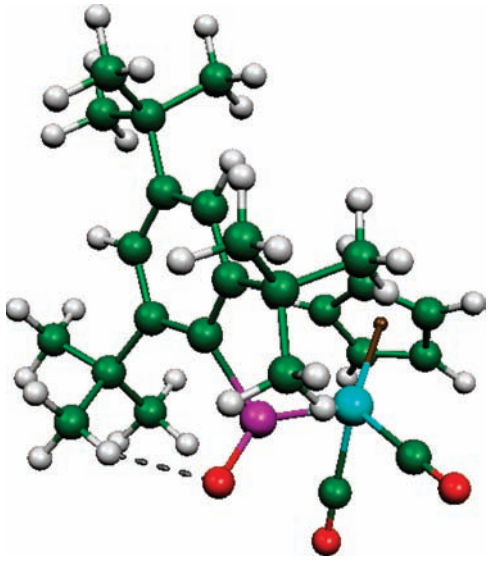

Figure 6. DFT-optimized structure of the anion $[MoCp\{P(O)R^*\}(CO)_2]^-$.

Table 5. Selected Atomic Charges in the Anion $[MoCp\{P(O)R^*\}(CO)_2]^-$

atom	Mulliken	NPA
Mo	1.64	−0.58
P	−0.98	1.41
O	−0.20	−1.07
C1	−0.50	0.57
C2	−0.46	0.56
O1	−0.22	−0.55
O2	−0.24	−0.55

already present in the free oxophosphinidene molecule (O····H = 2.281 Å). In contrast, in the real salt **3** this moderate interaction is overridden by the much stronger hydrogen bonding (O···H = 1.524 Å) with the H(N) atom of the cation.

The atomic charges computed for the anion in **3** are collected in the Table 5, these including Mulliken charges,[32] and those derived from the NBO analysis (NPA charges).[33] The first scheme of charges in this case yields values that must be considered unrealistic, since it places, for instance, a negative charge on C higher than that on O in the carbonyl ligands. This problem is a well established limitation of the Mulliken partitioning scheme, which in the presence of diffuse functions can lead to absurd behaviors.[31] The NPA charges give possibly in this case a more realistic picture of the local balance of charges, and yields the highest negative charge (−1.07*e*) at the O atom of the oxophosphinidene ligand, it being followed by charges of about −0.5*e* at the Mo atom and the O atoms of the carbonyl ligands, the latter being sensible values for a transition-metal carbonyl anion. From these figures we could predict that, under conditions of charge control, an electrophile would rather attack the O atom of the oxophosphinidene ligand, thus explaining the

(29) (a) Koch, W.; Holthausen, M. C. *A Chemist's Guide to Density Functional Theory*, 2nd ed.; Wiley-VCH: Weinheim, 2002. (b) Ziegler, T. *Chem. Rev*. **1991**, *91*, 651. (c) Foresman, J. B.; Frisch, ó. *Exploring Chemistry with Electronic Structure Methods*, 2nd ed.; Gaussian, Inc.: Pittsburg, 1996.

(30) Bader, R. F. W. *Atoms in molecules-A Quantum Theory*; Oxford University Press: Oxford, U. K., 1990.

(31) Cramer, C. J. *Essentials of Computational Chemistry*, 2nd ed.; Wiley: Chichester, U.K., 2004.

(32) Mulliken, R. S. *J. Chem. Phys*. **1955**, *23*, 1833.

(33) Mulliken population analysis fails to give a useful and reliable characterization of the charge distribution in many cases, especially when highly ionic compounds and diffuse basis functions are involved. Charges calculated according to the natural population analysis (NPA) do not show these deficiencies and are more independent of the basis set: (a) Reed, A. E.; Weinstock, R. B.; Weinhold, F. *J. Chem. Phys*. **1985**, *83*, 735. (b) Reed, A. E.; Curtis, L. A.; Weinhold, F. *Chem. Rev*. **1988**, *88*, 899.

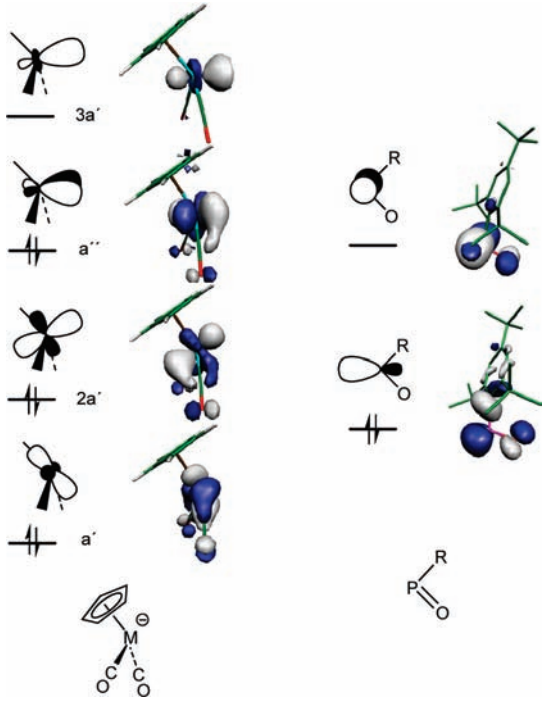

Figure 7. Idealized[32,1a] and DFT-computed frontier orbitals in the $[MoCpCO)_2]^-$ (left) and P(O)R* (right) fragments, depicted in order of increasing energy (not scaled, see text).

formation of the hydroxyphosphide compounds **4** and **4′** following the attack of the hardest acid (H^+), and that of the alkoxyphosphide products **8a**−**d** upon reaction with electrophilic reagents having a high positive charge placed at carbon, such as $[Me_3O][BF_4]$, Et_2SO_4, and acid chlorides. In contrast, the reactions of **3** with mild electrophilic reagents, having a less positively charged acceptor atom, must follow from suitable orbital interactions of the acceptor with the highest occupied molecular orbitals of the anion (orbital control).

Following earlier calculations on generic $MCp(CO)_2$ (under C_{2v} symmetry) and P(O)R fragments,[34,1a,3] we might anticipate that the binding between the $MoCp(CO)_2$ and P(O)R* fragments in the anion **3** should be made up of two main interactions, a σ donation from the lone pair on P to the lowest-energy empty orbital at Mo (3a′) and a π backbonding interaction from a suitably oriented and filled orbital at Mo (a″) to the empty p orbital at phosphorus (Figure 7). The latter interaction would explain the experimental conformation of the oxophosphinidene ligand in **3**, close to the plane bisecting the $MoCp(CO)_2$ fragment to maximize this orbital overlap. A DFT calculation of the actual fragments in the anion **3** gives a similar picture for the relevant frontier orbitals (Figure 7), although there is some mixing with the π*(CO) orbitals in the case of the metal fragment and significant π*(PO) character in the lowest unoccupied molecular orbital (LUMO) of the free oxophosphinidene molecule.

The most relevant Kohn−Sham molecular orbitals in the DFT-optimized anion $[MoCp(CO)_2\{P(O)R^*\}]^-$ are depicted in the Figure 8, along with their associated

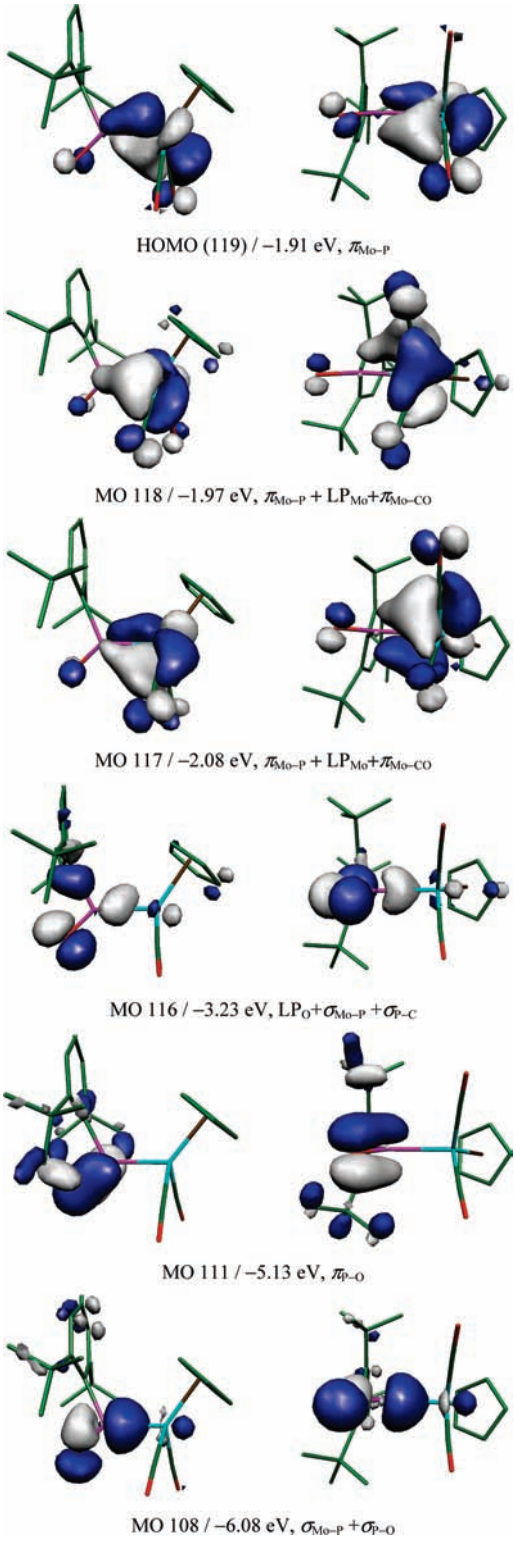

Figure 8. Selected DFT-computed molecular orbitals of the anion $[MoCp\{P(O)R^*\}(CO)_2]^-$, with their energies and main bonding character indicated below, shown in two different views.

energy and prevalent bonding character. As predicted, there is substantial π overlap between metal-based orbitals and phosphorus, but rather than restricted to one molecular orbital (the one arising from the 3a′ metal-based orbital, actually the highest occupied molecular orbital (HOMO) of the molecule) there is also significant π overlap in the two orbitals placed just below (MOs 118 and 117).

(34) Schilling, B. E. R.; Hoffmann, R.; Litchtenberger, D. L. *J. Am. Chem. Soc.* **1979**, *101*, 585.

The latter can be viewed as arising from the ideal a′ and 2a′ orbitals of the metal fragment, and would be strictly nonbonding in an ideal geometry with the P(O)R ligand placed in the bisecting plane of the metal fragment. However, as stated above, the oxophosphinidene plane is slightly twisted with respect to that bisecting plane (ca. 12° in the DFT-optimized geometry), and this allows nonzero overlaps between the LUMO of the oxophosphinidene and the three a′-type orbitals of the Mo fragment, while at the same time strengthening the hydrogen bonding between the oxygen and the closer *ortho*-^{t}Bu group of the oxophosphinidene ligand. The three MOs thus formed are very close in energy (ca. −2 eV) and should account for the reactivity of the anion under conditions of orbital control, that is in the reactions with the milder electrophilic reagents. This is therefore consistent with the outcome of the reactions of **3** with alkyl halides to give phosphinite derivatives resulting from the binding of the hydrocarbon fragment to the phosphorus atom, although from the initial acid−base interaction we could not anticipate whether the hydrocarbon fragment would finally end up attached to phosphorus or to the metal atom. Actually, our preliminary study on the acid−base chemistry of the anion **3** revealed that the incoming electrophile might also end up bound to the metal atom,[6a] a behavior to be examined more in depth separately. In contrast, the MO 116, placed some 1.2 eV below the above frontier orbitals, has significant lone-pair character of the O atom of the oxophosphinidene ligand, and it would be the orbital accounting for the attachment of the incoming electrophile to the O atom, favored on electrostatic grounds as discussed above. Finally we note the presence of MO 111, with a preeminent π_{P-O} bonding nature, indicative of the retention of a substantial double-bond character in the oxophosphinidene ligand upon coordination to the metal, in spite of the π^*(PO) antibonding nature of the LUMO of the ligand.

Since the Mo−P and P−O π overlaps are mutually competitive (a strengthening in one should weaken the other) it is difficult from the above MO analysis to ascertain the relative strengths of these two interactions. We have shown previously that the analysis of the electron density under the AIM theory provides valuable information (complementary to that of the MO analysis) concerning the bonding in different metal complexes with CO, Cp, and P-donor ligands.[35−37] We have performed a similar analysis on the anion in **3**, and also on the free ligand, with the values of the electron density (ρ) and its Laplacian ($\nabla^2\rho$) at the most relevant bond critical points (bcp) being collected in the Table 6. The free phosphinidene molecule displays a high electron density at the P−O bcp (1.472 e Å^{-3}; P−O = 1.501 Å), consistent with a substantial double-bond character. Note also the very high value of its Laplacian (ca. 33 e Å^{-5}) a feature characteristic of multiple CO bonds in organic molecules and transition-metal carbonyls.[38] Upon coordination of the oxophosphinidene ligand, both parameters are reduced as expected, but only to a small extent, this suggesting that the P−O bond in the anion keeps most of its multiplicity, in agreement with the nature of the MO 111 orbital and the short experimental distance of this bond. At the same time, the newly formed Mo−P bond displays topological properties indicative of substantial multiplicity too. Thus, both the electron density and its Laplacian at the corresponding bcp (0.636 e Å^{-3} and 5.54 e Å^{-5} respectively) are substantially higher than the values computed for the single/dative Mo−P bonds in several PCy_2-bridged complexes (ca. 0.53 e Å^{-3} and 3 e Å^{-5}),[35b,36,37] and comparable to those recently computed for the essentially double Mo−P bond in the phosphinidene-bridged complex [$Mo_2Cp_2(\mu$-PH)$(CO)_2(\eta^6$-R*H)] (0.654 e Å^{-3} and 4.49 e Å^{-5}, respectively).[39] In summary, taking together the information derived from the preceding MO and AIM analysis, we can conclude that the Mo−P binding in the oxophosphinidene complex **3** has a strong π component and must therefore be described as close to a double bond, whereas the P−O bond within the oxophosphinidene group retains most of the multiplicity present in the free ligand.

Table 6. Topological Properties of the Electron Density.[a]

bond	ρ	$\nabla^2(\rho)$
	Free P(O)R*	
P−O	1.472	33.27
P−C(aryl)	1.061	−7.11
	[MoCp{P(O)R*}$(CO)_2$]$^-$	
Mo−P	0.636	5.54
P−O	1.431	29.38
P−C(aryl)	0.977	−6.00
Mo−C1	0.890	11.65
C1−O1	2.997	7.27
Mo−C2	0.873	11.50
C2−O2	2.998	7.33

[a] Values of the electron density at the bond critical points (ρ) are given in e Å^{-3}; values of the Laplacian of ρ at these points ($\nabla^2\rho$) are given in e Å^{-5}.

Concluding Remarks

The reactions of the binuclear complexes (H-DBU)[$M_2Cp_2(\mu$-PHR*$)(CO)_4$] with O_2 yield the corresponding mononuclear derivatives (H-DBU)[MCp{P(O)R*}$(CO)_2$] (M = Mo (**3**), W (**3′**)), these being the first anionic oxophosphinidene complexes described in the literature. According to the experimental data and DFT calculations on the Mo anion, the binding of the oxophosphinidene ligand to the metal center has a strong π component, described by the highest occupied MOs, and therefore can be properly described as a double bond. These molecular orbitals should account for the reactivity of the anion under conditions of orbital control, it being consistent with the outcome of the reactions of **3** with mild electrophilic reagents such as alkyl halides to give phosphinite derivatives [MoCp{κ^2-OP(R)R*}$(CO)_2$] resulting from the binding of the hydrocarbon fragment to the phosphorus atom of the anion. The P−O bond of the oxophoshinidene ligand is relatively unperturbed upon coordination to the metal center, and in the anionic

(35) (a) García, M. E.; García-Vivó, D.; Ruiz, M. A.; Alvarez, S.; Aullón, G. *Organometallics* **2007**, *26*, 4930. (b) García, M. E.; García-Vivó, D.; Ruiz, M. A.; Alvarez, S.; Aullón, G. *Organometallics* **2007**, *26*, 5912.

(36) García, M. E.; Ramos, A.; Ruiz, M. A.; Lanfranchi, M.; Marchio, L. *Organometallics* **2007**, *26*, 6197.

(37) García, M. E.; García-Vivó, D.; Melón, S.; Ruiz, M. A.; Graiff, C.; Tiripicchio, A. *Inorg. Chem.* **2009**, *48*, 9282.

(38) Macchi, P.; Sironi, A. *Coord. Chem. Rev.* **2003**, *238−239*, 383.

(39) Alvarez, M. A.; Amor, I.; García, M. E.; García-Vivó, D.; Ruiz, M. A.; Suárez, J. *Organometallics* **2010** (in press, ref. om-2010-00529a).

complex its oxygen atom bears the highest negative charge, and therefore it should be the active site of the anions **3** and **3′** under conditions of charge control, thus explaining the formation of the hydroxyphosphide compounds $[MCp\{P(OH)R^*\}(CO)_2]$ following the attack of protic acids, and that of the alkoxyphosphide products $[MoCp\{P(OR)R^*\}(CO)_2]$ upon reaction with electrophilic reagents having a high positive charge placed at carbon.

Experimental Section

General Procedures and Starting Materials. All manipulations and reactions were carried out under a nitrogen (99.995%) atmosphere using standard Schlenk techniques. Solvents were purified according to literature procedures,[40] and distilled prior to use. Petroleum ether refers to that fraction distilling in the range 338−342 K. Compounds **1**,[7] $[Mo_2Cp_2(CO)_4]$,[41] $[W_2Cp_2(CO)_4]$,[41] and $[Li(THF)_3][PHR^*]$ ($R^* = 2,4,6\text{-}C_6H_2{}^tBu_3$),[42] were prepared as described previously. All other reagents were obtained from the usual commercial suppliers and used as received. Chromatographic separations were carried out using jacketed columns cooled by tap water (ca. 288 K). Commercial aluminum oxide (activity I, 150 mesh) was degassed under vacuum prior to use. The latter was mixed under nitrogen with the appropriate amount of water to reach the activity desired. Filtrations were performed using diatomaceous earth. IR stretching frequencies of CO ligands were measured typically in solution. Nuclear Magnetic Resonance (NMR) spectra were routinely recorded at 300.13 (^1H), 121.50 ($^{31}P\{^1H\}$), or 75.47 MHz ($^{13}C\{^1H\}$) at 290 K in CD_2Cl_2 solutions unless otherwise stated. Chemical shifts (δ) are given in parts per million (ppm), relative to internal tetramethylsilane (TMS) or external 85% aqueous H_3PO_4 solutions (^{31}P). Coupling constants (J) are given in hertz. The aromatic ^{13}C NMR resonances for the aryl group are reported as $C^n(R^*)$, (n = 1 to 6), and those of the ^{t}Bu groups as $C^n(^tBu)$ (n = 1, 2).

Preparation of $[W_2Cp_2(\mu\text{-}H)(\mu\text{-}PHR^*)(CO)_4]$ (1′). A diglyme solution (30 mL) containing about 0.75 mmol of $[W_2Cp_2(CO)_4]$ was prepared in situ from $[W_2Cp_2(CO)_6]$ and was transferred using a canula over solid $[Li(THF)_3][PHR^*]$ (0.71 mmol) freshly prepared. The mixture was then stirred for 10 min to yield a dark green solution of the Li^+ salt of the anionic complex $[W_2Cp_2(\mu\text{-}PHR^*)(CO)_4]^-$. Aqueous 85% H_3PO_4 (0.2 mL, excess) was then added, and the mixture was stirred for 5 min to give a deep red solution. Removal of the solvent under vacuum gave a residue which was extracted with dichloromethane−petroleum ether (1:1) and filtered. Removal of solvents from the filtrate gave a residue which was then dissolved in the minimum amount of dichloromethane and chromatographed on alumina (activity IV, 40 × 4 cm). Elution with dichloromethane−petroleum ether (1:4) gave a red band. Removal of the solvents from the latter fraction yielded compound **1′** as a red microcrystalline solid (0.378 g, 57%). Anal. Calcd for $C_{32}H_{41}O_4PW_2$: C, 43.27; H, 4.65. Found: C, 43.38; H, 4.64. ^1H NMR (400.13 MHz, $CDCl_3$): δ 8.88 (d, J_{HP} = 373, 1H, PH), 7.33 (d, J_{HP} = 3, 2H, C_6H_2), 5.42 (s, br, 10H, Cp), 1.46 (s, 18H, *o*-^{t}Bu), 1.30 (s, 9H, *p*-^{t}Bu), −16.27 [d, J_{HP} = 25, J_{HW} = 42, 1H, μ-H]. $^{13}C\{^1H\}$ NMR (100.62 MHz, $CDCl_3$): δ 229.0 (s, br, 4CO), 155.8 [s, J_{CP} = 21, $C^2(R^*)$], 149.1 [s, $C^4(R^*)$], 132.3 [d, J_{CP} = 24, $C^1(R^*)$], 122.4 [d, J_{CP} = 10, $C^3(R^*)$], 89.8 (s, br, Cp), 38.6 [s, C^1(*o*-^{t}Bu)], 34.6 [s, C^1(*p*-^{t}Bu)], 34.4 [s, br, C^2(*o*-^{t}Bu)], 31.0 [s, C^2(*p*-^{t}Bu)].

Preparation of Solutions of (H-DBU)$[Mo_2Cp_2(\mu\text{-}PHR^*)(CO)_4]$ (2). Neat 1,8-diazabicyclo [5.4.0] undec-7-ene (DBU, 48 μL, 0.321 mmol) was added to a solution of compound **1** (0.150 g, 0.211 mmol) in THF or dichloromethane (40 mL) at 273 K, and the mixture was stirred at that temperature for 3 h to give a green solution shown (by IR and ^{31}P NMR spectroscopy) to contain essentially pure compound **2**, which was ready for further use. All attempts to isolate this compound as a crystalline material from these solutions led to its progressive decomposition.

Preparation of Solutions of (H-DBU)$[W_2Cp_2(\mu\text{-}PHR^*)(CO)_4]$ (2′). Neat DBU (38 μL, 0.252 mmol) was added to a solution of compound **1** (0.150 g, 0.169 mmol) in THF or dichloromethane (40 mL) at 273 K, and the mixture was stirred at that temperature for 4 h to give a green solution shown (by IR and ^{31}P NMR spectroscopy) to contain essentially pure compound **2′**, as a mixture of *cis* and *trans* isomers, which was ready for further use. All attempts to isolate this compound as a crystalline material from these solutions led to its progressive decomposition. ^1H NMR (203 K): Isomer *trans*: δ 5.36 (s, 5H, Cp), 5.13 (s, 5H, Cp); Isomer *cis*: δ 5.26 (s, 10H, Cp), other resonances could not be assigned separately to each isomer. Ratio *cis*/*trans*: 1/3.

Preparation of (H-DBU)$[MoCp\{P(O)R^*\}(CO)_2]$ (3). Neat DBU (95 μL, 0.632 mmol) was added to a dichloromethane solution (30 mL) of $[Mo_2Cp_2(\mu\text{-}H)(\mu\text{-}PHR^*)(CO)_4]$ (**1**) (0.300 g, 0.421 mmol), and the mixture was stirred at 273 K for 3 h to give a dark green solution of the salt **2**. Air (70 mL, ca. 0.61 mmol) was then injected into the solution using a syringe, the Schlenk tube was closed, and the mixture was stirred at 258 K for 5 h to give an orange solution. The solvent was then removed under vacuum, the residue was extracted with diethylether, and the extracts were filtered. The solvent was then removed from the filtrate, and the residue was crystallized by slow diffusion of layers of diethyl ether and petroleum ether into a concentrated solution of the crude material in toluene. This yielded compound **3** as yellow crystals (0.171 g, 61%). Anal. Calcd for $C_{34}H_{51}MoN_2O_3P$: C, 61.62; H, 7.76; N, 4.23. Found: C, 61.51; H, 7.77; N, 4.25. ^1H NMR (200.13 MHz, C_6D_6): δ 13.88 (s, 1H, NH), 7.52 (s, 2H, C_6H_2), 5.11 (s, 5H, Cp), 3.31, 2.72, 2.15, 1.99, 1.51, 1.12, 1.02, 0.70 (8 m, 8 × 2H, CH_2), 2.03 (s, 18H, *o*-^{t}Bu), 1.37 (s, 9H, *p*-^{t}Bu). $^{13}C\{^1H\}$ NMR δ 240.8 (d, J_{CP} = 21, CO), 166.2 (s, CN), 155.9 [d, J_{CP} = 30, $C^1(R^*)$], 148.4 [s, $C^4(R^*)$], 146.4 [d, J_{CP} = 6, $C^2(R^*)$], 121.6 [d, J_{CP} = 4, $C^3(R^*)$], 90.7 (s, Cp), 54.5, 48.7, 38.4, 32.3, 29.2, 27.0, 24.2, 19.7 (8s, CH_2), 38.43 [s, C^1(*o*-^{t}Bu)], 34.7 [s, C^1(*p*-^{t}Bu)], 34.3 [s, C^2(*o*-^{t}Bu)], 30.9 [s, C^2(*p*-^{t}Bu)].

Preparation of (H-DBU)$[WCp\{P(O)R^*\}(CO)_2]$ (3′). Neat DBU (76 μL, 0.505 mmol) was added to a CH_2Cl_2 solution (40 mL) of $[W_2Cp_2(\mu\text{-}H)(\mu\text{-}PHR^*)(CO)_4]$ (**1′**) (0.300 g, 0.338 mmol), and the mixture was stirred at 273 K for 4 h to give a dark green solution of the salt **2′**. Air (60 mL, ca. 0.53 mmol) was then injected to the solution cooled at 253 K using a syringe, the Schlenk tube was closed, and the mixture was stirred for 5 h to give an orange solution. Workup as described for **3** yielded compound **3′** as yellow crystals (0.150 g, 59%). Anal. Calcd for $C_{34}H_{51}N_2O_3PW$: C, 54.41; H, 6.85; N, 3.73. Found: C, 54.50; H, 6.77; N, 3.65. ^1H NMR: δ 12.43 (s, 1H, NH), 7.28 (s, 2H, C_6H_2), 4.80 (s, 5H, Cp), 3.50−3.41 (m, 6H, CH_2), 2.92, 2.02 (2 m, 2 × 2H, CH_2), 1.86−1.71 (m, 6H, CH_2), 1.61 (s, 18H, *o*-^{t}Bu), 1.31 (s, 9H, *p*-^{t}Bu).

Preparation of $[MoCp\{P(OH)R^*\}(CO)_2]$ (4). Neat $HBF_4\cdot OEt_2$ (6 μL of a 54% solution in Et_2O, 0.045 mmol) was added to a dichloromethane (10 mL) solution of compound **3** (0.030 g, 0.045 mmol) to give instantaneously an orange solution. The solvent was then removed under vacuum, the residue was extracted with toluene, and the extracts were filtered. Removal of the solvent from the filtrate gave an orange residue shown (by IR and ^{31}P NMR) to contain compound **4** (0.018 g, 78%) as the major species. All attempts to further purify this crude material led to its progressive decomposition. ^1H NMR: δ 7.44 (d, J_{HP} = 3, 2H, C_6H_2), 6.26 (s, 1H, OH), 5.24 (s, 5H, C_5H_5), 1.65 (s, 18H, *o*-^{t}Bu), 1.32 (s, 9H, *p*-^{t}Bu).

(40) Perrin, D. D.; Armarego, W. L. F. *Purification of Laboratory Chemicals*; Pergamon Press: Oxford, U. K., 1988.
(41) Curtis, M. D.; Hay, M. S. *Inorg. Synth.* **1990**, *28*, 152.
(42) (a) Cowley, A. H.; Kilduff, J. E.; Newman, T. H.; Pakulski, M. *J. Am. Chem. Soc.* **1982**, *104*, 5820. (b) Hou, Z.; Breen, T. L.; Stephan, D. W. *Organometallics* **1993**, *12*, 3158.

Preparation of [WCp{P(OH)R*}(CO)$_2$] (4′). Neat $HBF_4 \cdot OEt_2$ (6 μL of a 54% solution in Et_2O, 0.045 mmol) was added to a dichloromethane (10 mL) solution of compound **3′** (0.030 g, 0.040 mmol) to give an orange solution instantaneously. The solvent was then removed under vacuum, the residue was extracted with toluene, and the extracts were filtered using a canula. Removal of the solvent from the filtrate gave an orange residue shown (by IR and ^{31}P NMR) to contain compound **4′** (0.017 g, 74%) as the major species. All attempts to further purify this crude material lead to its progressive decomposition.

Preparation of [MoCp(PFR*)(CO)$_2$] (5). Neat $HBF_4 \cdot OEt_2$ (13 μL of a 54% solution in Et_2O, 0.094 mmol) was added to a dichloromethane solution (10 mL) of compound **3** (0.030 g, 0.045 mmol) at 273 K to give an orange solution instantaneously. The solvent was then removed under vacuum, the residue was extracted with petroleum ether, and the extracts were filtered. The solvent was then partially removed under vacuum from the filtrate, and the concentrated solution was allowed to crystallize at 253 K to give compound **5** as red-purple crystals (0.018 g, 80%) suitable for X-ray diffraction studies. Anal. Calcd for $C_{25}H_{34}FMoO_2P$: C, 58.59; H, 6.69. Found: C, 58.21; H, 6.52. ^{1}H NMR (200.13 MHz): δ 7.45 (d, J_{HP} = 3, 2H, C_6H_2), 5.35 (s, 5H, Cp), 1.63 (s, 18H, *o*-^{t}Bu), 1.32 (s, 9H, *p*-^{t}Bu). ^{13}C{^{1}H} NMR: δ 236.0 (dd, J_{CP} = 25, J_{CF} = 3, CO), 153.6 [s, C^4(R*)], 151.9 [d, J_{CP} = 5, C^2(R*)], 144.9 [d, J_{CP} = 24, C^1(R*)], 123.0 [d, J_{CP} = 8, C^3(R*)], 94.0 (s, Cp), 38.4 [s, C^1(*o*-^{t}Bu)], 35.5 [s, C^1(*p*-^{t}Bu)], 34.1 [s, C^2(*o*-^{t}Bu)], 31.1 [s, C^2(*p*-^{t}Bu)].

Preparation of [WCpCl{PH(OH)R*}(CO)$_2$] (7). Hydrogen chloride (80 μL of a 3.2 M solution in Et_2O, 0.26 mmol) was added to a dichloromethane solution (10 mL) of compound **3′** (0.060 g, 0.09 mmol) at 273 K to give instantaneously a red solution, and the mixture was stirred for 10 min to give a mixture of the compounds [WCpCl{PHClR*}(CO)$_2$] (**6**) (major) and **7** (minor) in variable relative amounts. Degassed water (12 μL, 0.67 mmol) was then added to the solution, and the mixture was further stirred for 10 min. Solvent was then removed under vacuum, the residue was extracted with petroleum ether, and the extracts were filtered with a canula. Removal of the solvent under vacuum gave a residue which was crystallized by the slow diffusion of a layer of toluene-petroleum ether (1:8) into a concentrated dichloromethane solution of the complex at 253 K. This gave compound **7** as red crystals (0.025 g, 50%) suitable for X-ray diffraction. All attempts to isolate compound **6** from the crude reaction mixture (before addition of water) caused its progressive transformation into **7** and other minor products. *Data for compound* ***6***: ^{1}H NMR: δ 8.64 (d, J_{HP} = 422, 1H, PH), 7.51 (d, J_{HP} = 3, 2H, C_6H_2), 5.59 (s, 5H, Cp), 1.56 (s, br, 18H, *o*-^{t}Bu), 1.32 (s, 9H, *p*-^{t}Bu). *Data for compound* *7*: Anal. Calcd for $C_{25}H_{34}O_3PW$: C, 50.27; H, 5.74. Found: C, 49.88; H, 5.60. ^{1}H NMR: δ 9.22 (dd, J_{HP} = 396, J_{HH} = 3, 1H, PH), 7.51, 7.43 (2s, br, 2 × 1H, C_6H_2), 7.11 (d, J_{HH} = 3, 1H, OH), 5.54 (s, 5H, Cp), 1.61, 1.46 (2s, br, 2 × 9H, *o*-^{t}Bu), 1.30 (s, 9H, *p*-^{t}Bu).

Preparation of [MoCp{P(OMe)R*}(CO)$_2$] (8a). A dichloromethane solution (10 mL) of compound **3** (0.030 g, 0.045 mmol) was stirred at 273 K with $[Me_3O]BF_4$ (0.010 g, 0.067 mmol) for 2 min to give an orange solution. The solvent was then removed under vacuum, the residue was extracted with CH_2Cl_2-petroleum ether (1:3), and the extracts were chromatographed on alumina (activity IV) at 288 K. Elution with the same solvent mixture gave an orange fraction. Removal of solvents from the latter gave compound **8a** as an orange solid (0.020 g, 84%). Anal. Calcd for $C_{26}H_{37}MoO_3P$: C, 59.54; H, 7.11. Found: C, 59.12; H, 6.95. ^{1}H NMR: δ 7.43 (d, J_{HP} = 3, 2H, C_6H_2), 5.14 (s, 5H, Cp), 3.98 [d, J_{HP} = 14, 3H, OCH_3], 1.57 (s, 18H, *o*-^{t}Bu), 1.32 (s, 9H, *p*-^{t}Bu). ^{13}C{^{1}H} NMR: δ 238.5 (d, J_{CP} = 20, CO), 152.2 [s, C^4(R*)], 150.2 [d, J_{CP} = 6, C^2(R*)], 145.0 [d, J_{CP} = 14, C^1(R*)], 123.3 [d, J_{CP} = 8, C^3(R*)], 93.0 (s, Cp), 55.7 (s, OCH_3), 39.0 [s, C^1(*o*-^{t}Bu)], 35.3 [s, C^1(*p*-^{t}Bu)], 34.3 [s, C^2(*o*-^{t}Bu)], 31.1 [s, C^2(*p*-^{t}Bu)].

Preparation of [MoCp{P(OEt)R*}(CO)$_2$] (8b). A dichloromethane solution (10 mL) of compound **3** (0.030 g, 0.045 mmol) was stirred at room temperature with Et_2SO_4 (60 μL, 0.449 mmol) for 2 h to give an orange solution. The solvent was then removed under vacuum, and the residue was dissolved in 1 mL of CH_2Cl_2 and chromatographed on alumina (activity IV) at 288 K. Elution with CH_2Cl_2-petroleum ether (1:3) gave an orange fraction. Removal of solvents from the latter gave compound **8b** as an orange solid (0.022 g, 90%). Anal. Calcd for $C_{27}H_{39}MoO_3P$: C, 60.22; H, 7.30. Found: C, 60.42; H, 7.52. ^{1}H NMR: δ 7.43 (d, J_{HP} = 3, 2H, C_6H_2), 5.11 (s, 5H, Cp), 4.40 (dq, J_{HH} = 7, J_{HP} = 7, 2H, CH_2), 1.57 (s, 18H, *o*-^{t}Bu), 1.41 (t, J_{HH} = 7, 3H, CH_2CH_3), 1.33 (s, 9H, *p*-^{t}Bu). ^{13}C{^{1}H} NMR: δ 238.1 (d, J_{CP} = 20, CO), 151.7 [s, C^4(R*)], 149.6 [d, J_{CP} = 6, C^2(R*)], 144.9 [d, J_{CP} = 13, C^1(R*)], 123.0, [d, J_{CP} = 8, C^3(R*)], 92.4 (s, Cp), 64.7 (s, OCH_2), 38.7 [s, C^1(*o*-^{t}Bu)], 34.9 [s, C^1(*p*-^{t}Bu)], 34.0 [s, C^2-(*o*-^{t}Bu)], 30.7 [s, C^2(*p*-^{t}Bu)], 15.5 [d, J_{CP} = 6, CH_2CH_3].

Preparation of [MoCp{P(OC(O)C$_2$H$_3$)R*}(CO)$_2$] (8c). A dichloromethane solution (10 mL) of compound **3** (0.036 g, 0.054 mmol) was stirred at room temperature with $C_2H_3C(O)Cl$ (18 μL, 0.216 mmol) for 15 min to give a purple solution. The solvent was then removed under vacuum, and the residue was extracted with toluene-petroleum ether (1:1). The extracts were filtered through alumina (activity IV, 10 × 2 cm). Removal of solvents from the filtrate gave compound **8c** as a purple solid (0.025 g, 80%). Anal. Calcd for $C_{28}H_{37}MoO_4P$: C, 59.57; H, 6.61. Found: C, 59.21; H, 6.40. ^{1}H NMR: δ 7.44 (d, J_{HP} = 3, 2H, C_6H_2), 6.49 (dd, J_{HH} = 17, J_{HH} = 1, 1H, *trans*-CH_2), 6.15 (dd, J_{HH} = 17, J_{HH} = 10, 1H, CH), 5.94 (dd, J_{HH} = 10, J_{HH} = 1, 1H, *cis*-CH_2), 5.22 (s, 5H, Cp), 1.60 (s, 18H, *o*-^{t}Bu), 1.33 (s, 9H, *p*-^{t}Bu). ^{13}C{^{1}H} NMR: δ 237.6 (d, J_{CP} = 23, CO), 162.2 [d, J_{CP} = 8, $C(O)C_2H_3$], 152.7 [s, C^4(R*)], 150.7 [d, J_{CP} = 5, C^2(R*)], 144.9 [d, J_{CP} = 12, C^1(R*)], 132.8 (s, CH_2), 129.6 (s, CH), 123.4 [d, J_{CP} = 8, C^3(R*)], 93.7 (s, Cp), 39.1 [s, C^1(*o*-^{t}Bu)], 35.3 [s, C^1(*p*-^{t}Bu)], 34.4 [s, C^2(*o*-^{t}Bu)], 31.1 [s, C^2(*p*-^{t}Bu)].

Preparation of [MoCp{P(OC(O)Ph)R*}(CO)$_2$] (8d). A dichloromethane solution (10 mL) of compound **3** (0.036 g, 0.054 mmol) was stirred with PhC(O)Cl (26 μL, 0.22 mmol) for 2 min. The solvent was then removed under vacuum to give a dark red residue which was extracted with petroleum ether. The extracts were filtered through alumina (activity IV, 2 cm), and the solvent was then removed from the filtrate to give compound **8d** as a purple solid (0.026 g, 78%). The crystals used in the X-ray study were grown by slow diffusion at 253 K of a layer of petroleum ether into a concentrated toluene solution of the complex. Anal. Calcd for $C_{32}H_{39}MoO_4P$: C, 62.54; H, 6.40. Found: C, 62.82; H, 6.58. ^{1}H NMR: δ 8.07 (m, 2H, Ph), 7.61 (m, 1H, Ph), 7.49−7.44 (m, 4H, Ph and C_6H_2), 5.24 (s, 5H, Cp), 1.62 (s, 18H, *o*-^{t}Bu), 1.35 (s, 9H, *p*-^{t}Bu). ^{13}C{^{1}H} NMR: δ 237.9 (d, J_{CP} = 23, CO), 162.9 [d, J_{CP} = 8, *C*(O)Ph], 152.8 [s, C^4(R*)], 150.7 [d, J_{CP} = 5, C^2(R*)], 145.0 [d, J_{CP} = 12, C^1(R*)], 133.8 [s, C^4(Ph)], 130.9 [s, C^1(Ph)], 130.5 [s, C^2(Ph)], 128.9 [s, C^3(Ph)], 123.5 [d, J_{CP} = 9, C^3(R*)], 93.8 (s, Cp), 39.2 [s, C^1(*o*-^{t}Bu)], 35.4 [s, C^1(*p*-^{t}Bu)], 34.4 [s, C^2(*o*-^{t}Bu)], 31.1 [s, C^2(*p*-^{t}Bu)].

Preparation of [MoCp(κ^2-OPMeR*)(CO)$_2$] (9a). Neat CH_3I (28 μL, 0.45 mmol) was added to a dichloromethane solution (10 mL) of compound **3** (0.030 g, 0.045 mmol), and the mixture was stirred at room temperature for 7 h to give a red solution. The solvent was then removed under vacuum, the residue was extracted with dichloromethane-petroleum ether (1:6), and the extracts were chromatographed on alumina (activity IV) at 288 K. A red fraction was eluted using the same solvent mixture yielding, after removal of solvents under vacuum, compound **9a** as a red solid (0.022 g, 92%). Anal. Calcd for $C_{26}H_{37}MoO_3P$: C, 59.54; H, 7.11. Found: C, 59.20; H, 7.52. ^{1}H NMR: δ 7.37−7.33 (m, ABX, 2H, C_6H_2), 5.01 (s, 5H, Cp), 2.17 [d, J_{HP} = 11, 3H, PCH_3), 1.64, 1.53, 1.31 (3s, 3 × 9H, ^{t}Bu). ^{13}C{^{1}H} NMR: δ 255.8 (d, J_{CP} = 26, CO), 246.0 (s, CO), 157.3 [d, J_{CP} = 18, $C^{2,6}$(R*)], 155.2 [s, C^4(R*)], 151.6 [s, $C^{6,2}$(R*)], 132.9 [d, J_{CP} = 34, C^1(R*)],

124.5 [d, J_{CP} = 8, $C^{3,5}$(R*)], 123.1 [d, J_{CP} = 14, $C^{5,3}$(R*)], 95.2 (s, Cp), 40.0, 39.3, 35.1 [3s, C^1(^{t}Bu)], 33.9, 33.2, 30.9 [3s, C^2-(^{t}Bu)], 23.8 [d, J_{CP} = 27, PCH_3].

Preparation of [MoCp(κ^2-OPEtR*)(CO)$_2$] (9b). Neat EtI (40 μL, 0.50 mmol) was added to a dichloromethane solution (10 mL) of compound **3** (0.030 g, 0.050 mmol), and the mixture was stirred at 303 K for 15 h to give a red solution. The solvent was then removed under vacuum, and the residue was chromatographed on alumina (activity IV) at 288 K. Elution with dichloromethane-petroleum ether (1:5) gave an orange fraction yielding, after removal of solvents under vacuum, compound **9b** as a red solid (0.023 g, 86%). Anal. Calcd for $C_{27}H_{39}MoO_3P$: C, 60.22; H, 7.30. Found: C, 59.84; H, 7.21. ^{1}H NMR (200.13 MHz): δ 7.39−7.35 (m, ABX, 2H, C_6H_2), 5.00 (s, 5H, Cp), 2.74 (m, 2H, CH_2), 1.64, 1.51, 1.31 (3s, 3 × 9H, ^{t}Bu), 0.94 (dt, J_{HP} = 20, J_{HH} = 7, 3H, CH_3). ^{13}C{^{1}H} NMR: δ 255.2 (d, J_{CP} = 27, CO), 247.2 (s, CO), 157.1, 151.3 [2d, J_{CP} = 18, J_{CP} = 4, $C^{2,6}$(R*)], 155.0 [s, C^4(R*)], 133.7 [d, J_{CP} = 27, C^1(R*)], 124.6 [d, J_{CP} = 9, $C^{3,5}$(R*)], 123.1 [d, J_{CP} = 14, $C^{5,3}$(R*)], 95.1 (s, Cp), 40.0, 39.4 [2d, J_{CP} = 2, *o*-C^1(^{t}Bu)], 35.1 [s, *p*-C^1(^{t}Bu)], 34.1, 33.2, 30.9 [3s, C^2(^{t}Bu)], 27.8 (d, J_{CP} = 25, PCH_2), 8.4 (s, CH_3).

Preparation of [MoCp{κ^2-OP(C_3H_5)R*}(CO)$_2$] (9e). The procedure is identical to that described for **9a**, but using allyl bromide (48 μL, 0.54 mmol) instead of MeI. After similar workup [elution with dichloromethane-petroleum ether (1:9)], compound **9e** was obtained as a bright-red solid (0.023 g, 84%). The crystals used in the X-ray study were grown by slow diffusion at 253 K of a layer of petroleum ether into a concentrated toluene solution of the complex. Anal. Calcd for $C_{28}H_{39}MoO_3P$: C, 61.09; H, 7.14. Found: C, 61.32; H, 7.42. ^{1}H NMR: δ 7.39−7.35 (m, ABX, 2H, C_6H_2), 5.55 (m, 1H, CH), 5.15 (m, 2H, CH_2), 5.00 (s, 5H, Cp), 3.52 (m, 2H, PCH_2), 1.65, 1.54, 1.31 (3s, 3 × 9H, ^{t}Bu). ^{13}C{^{1}H} NMR: δ 255.6 (d, J_{CP} = 27, CO), 246.5 (s, CO), 157.4 [d, J_{CP} = 19, $C^{2,6}$(R*)], 155.2 [s, C^4(R*)], 151.6 [d, J_{CP} = 4, $C^{6,2}$(R*)], 133.7 [d, J_{CP} = 23, C^1(R*)], 130.2 (d, J_{CP} = 7, CH), 124.6 [d, J_{CP} = 8, $C^{3,5}$(R*)], 123.3 [d, J_{CP} = 13. $C^{5,3}$(R*)], 119.9 (d, J_{CP} = 13, CH_2), 95.1 (s, Cp), 40.3 [s, C^1(^{t}Bu)], 40.0 (d, J_{CP} = 20, PCH_2), 39.4 [d, J_{CP} = 3, C^1(^{t}Bu)], 35.1 [s, C^1(^{t}Bu)], 34.1, 33.4, 31.0 [3s, C^2(^{t}Bu)].

Preparation of [MoCp{κ^2-OP(C_3H_3)R*}(CO)$_2$] (9f). The procedure is identical to that described for **9a**, but using propargyl bromide (48 μL, 0.43 mmol) instead of MeI, and a reaction time of 4 h. After similar workup [elution with dichloromethane-petroleum ether (1:3)], compound **9f** was obtained as a cherry-red solid (0.019 g, 70%). Anal. Calcd for $C_{28}H_{37}MoO_3P$: C, 61.31; H, 6.80. Found: C, 61.63; H, 6.64. ^{1}H NMR (200.13 MHz): δ 7.42−7.37 (m, ABX, 2H, C_6H_2), 5.05 (s, 5H, Cp), 3.56 (dd, J_{HP} = 5, J_{HH} = 3, 1H, CH_2), 3.51 (d, J_{HH} = 3, 1H, CH), 2.24 (dt, J_{HP} = 6, J_{HH} = 3, 1H, CH_2), 1.66, 1.54, 1.31 (3s, 3 × 9H, ^{t}Bu). ^{13}C{^{1}H} NMR: δ 255.6 (d, J_{CP} = 27, CO), 245.4 (s, CO), 157.6 [d, J_{CP} = 20, $C^{2,6}$(R*)], 152.2 [d, J_{CP} = 3, $C^{6,2}$(R*)], 155.3 [s, C^4(R*)], 131.6 [d, J_{CP} = 25, C^1(R*)], 124.7 [d, J_{CP} = 8, $C^{3,5}$(R*)], 123.6 [d, J_{CP} = 14, $C^{5,3}$(R*)], 95.3 (s, Cp), 77.6 [d, J_{CP} = 9, CH_2CCH], 73.0 [d, J_{CP} = 9, CH_2CCH], 39.9 [s, C^1(^{t}Bu)], 39.4 [d, J_{CP} = 3, C^1(^{t}Bu)], 35.09 [s, C^1(^{t}Bu)], 33.8, 33.1, 30.9 [3s, C^2(^{t}Bu)], 27.1 (d, J_{CP} = 18, CH_2CCH).

Table 7. Crystal Data for Compound **7**

mol formula	$C_{25}H_{36}ClO_3PW$
mol wt	634.81
cryst syst	monoclinic
space group	$P2_1/c$
radiation (λ, Å)	0.71073
a, Å	19.021(6)
b, Å	11.003(3)
c, Å	12.516(4)
α, deg	90
β, deg	90.019(5)
γ, deg	90
V, Å^3	2619.4(14)
Z	4
calcd density, gcm^{-3}	1.61
absorpt. coeff., mm^{-1}	4.596
temperature, K	120.0(1)
θ range (deg)	1.07 to 27.18
index ranges (*h*, *k*, *l*)	−24, 24; 0, 14; 0, 16
reflections collected	24499
independent refln. (R_{int})	5083(0.0874)
refln. with $I > 2\sigma(I)$	3501
R indexes[a] [data with $I > 2\sigma(I)$]	R_1 = 0.052 wR_2 = 0.120[b]
R indexes[a] (all data)	R_1 = 0.0747 wR_2 = 0.132[b]
GOF	0.926
restraints/parameters	3/297
$\Delta\rho$(max, min), e Å^{-3}	2.37, −3.456

[a] $R = \sum||F_o| - |F_c||/\sum|F_o|$; $wR = [\sum w(F_o^2 - F_c^2)^2/\sum w|F_o|^2]^{1/2}$; $w = 1/[\sigma^2(F_o^2) + (aP)^2 + bP]$ where $P = (F_o^2 + 2F_c^2)/3$. [b] a = 0.0715, b = 0.0000.

Computational Details. All computations described in this work were carried out using the GAUSSIAN03 package,[43] in which the hybrid method B3LYP was applied with the Becke three parameters exchange functional[44] and the Lee−Yang−Parr correlation functional.[45] Effective core potentials (ECP) and their associated double-ζ LANL2DZ basis set were used for the Mo atom.[46] The light elements (P, O, C, and H) were described with 6-311+G* basis set.[47] The diffuse and polarization functions of this basis set are required to better describe the diffuse electron density in the anion. Geometry optimizations were performed under no symmetry restrictions, using initial coordinates derived from X-ray data of the complex, and frequency analysis were performed to ensure that a minimum structure with no imaginary frequencies was achieved in each case. Molecular orbitals and vibrational modes were visualized using the Molekel program.[48] The topological analysis of the electron density (ρ) was carried out with the Xaim routine.[49]

X-ray Structure Determination for Compound 7. The X-ray intensity data were collected on a Smart-CCD-1000 Bruker diffractometer using graphite-monochromated Mo−K_α radiation at 120 K. Cell dimensions and orientation matrices were initially determined from least-squares refinements on reflections measured in 3 sets of 30 exposures collected in 3 different ω regions and eventually refined against all reflections. The software

(43) Frisch, M. J.; Trucks, G. W.; Schlegel, H. B.; Scuseria, G. E.; Robb, M. A.; Cheeseman, J. R.; Montgomery, Jr., J. A.; Vreven, T.; Kudin, K. N.; Burant, J. C.; Millam, J. M.; Iyengar, S. S.; Tomasi, J.; Barone, V.; Mennucci, B.; Cossi, M.; Scalmani, G.; Rega, N.; Petersson, G. A.; Nakatsuji, H.; Hada, M.; Ehara, M.; Toyota, K.; Fukuda, R.; Hasegawa, J.; Ishida, M.; Nakajima, T.; Honda, Y.; Kitao, O.; Nakai, H.; Klene, M.; Li, X.; Knox, J. E.; Hratchian, H. P.; Cross, J. B.; Bakken, V.; Adamo, C.; Jaramillo, J.; Gomperts, R.; Stratmann, R. E.; Yazyev, O.; Austin, A. J.; Cammi, R.; Pomelli, C.; Ochterski, J. W.; Ayala, P. Y.; Morokuma, K.; Voth, G. A.; Salvador, P.; Dannenberg, J. J.; Zakrzewski, V. G.; Dapprich, S.; Daniels, A. D.; Strain, M. C.; Farkas, O.; Malick, D. K.; Rabuck, A. D.; Raghavachari, K.; Foresman, J. B.; Ortiz, J. V.; Cui, Q.; Baboul, A. G.; Clifford, S.; Cioslowski, J.; Stefanov, B. B.; Liu, G.; Liashenko, A.; Piskorz, P.; Komaromi, I.; Martin, R. L.; Fox, D. J.; Keith, T.; Al-Laham, M. A.; Peng, C. Y.; Nanayakkara, A.; Challacombe, M.; Gill, P. M. W.; Johnson, B.; Chen, W.; Wong, M. W.; Gonzalez, C.; and Pople, J. A. *Gaussian 03*, Revision B.02; Gaussian, Inc.: Wallingford, CT, 2004.

(44) Becke, A. D. *J. Chem. Phys.* **1993**, *98*, 5648.

(45) Lee, C.; Yang, W.; Parr, R. G. *Phys. Rev. B* **1988**, *37*, 785.

(46) Hay, P. J.; Wadt, W. R. *J. Chem. Phys.* **1985**, *82*, 299.

(47) (a) Hariharan, P. C.; Pople, J. A. *Theor. Chim. Acta* **1973**, *28*, 213. (b) Petersson, G. A.; Al-Laham, M. A. *J. Chem. Phys.* **1991**, *94*, 6081. (c) Petersson, G. A.; Bennett, A.; Tensfeldt, T. G.; Al-Laham, M. A.; Shirley, W. A.; Mantzaris, J. *J. Chem. Phys.* **1988**, *89*, 2193.

(48) *MOLEKEL: An Interactive Molecular Graphics Tool*; Portmann, S.; Lüthi, H. P. *Chimia* **2000**, *54*, 766.

(49) Ortiz, J. C.; Bo, C. *Xaim*; Departamento de Química Física e Inorgánica, Universidad Rovira i Virgili: Tarragona, Spain, 1998.

SMART[50] was used for collecting frames of data, indexing reflections, and determining lattice parameters. The collected frames were then processed for integration by the software SAINT,[50] and a multiscan absorption correction was applied with SADABS.[51] Using the program suite WinGX,[52] the structure was solved by Patterson interpretation and phase expansion, and refined with full-matrix least-squares on F^2 using SHELXL97.[53] All non-hydrogen atoms were refined by full-matrix least-squares using anisotropic thermal parameters. All hydrogen atoms were fixed at calculated geometric positions in the last least-squares refinements, except for H1 (P−H) and H2 (O−H) which were located in the Fourier map; however, to refine H2 it was necessary to apply restraints on the H2−O3 length and the H2−O3−P1 angle. All hydrogen atoms were given an overall isotropic thermal parameter. Crystallographic data and structure refinement details for **7** are collected in the Table 7.

(50) *SMART & SAINT Software Reference Manuals, Version 5.051 (Windows NT Version)*; Bruker Analytical X-ray Instruments: Madison, WI, 1998.
(51) Sheldrick, G. M. *SADABS, Program for Empirical Absorption Correction*; University of Göttingen: Göttingen, Germany, 1996.
(52) Farrugia, L. J. *J. Appl. Crystallogr.* **1999**, *32*, 837.
(53) Sheldrick, G. M. *Acta Crystallogr., Sect. A* **2008**, *64*, 112.

Acknowledgment. We thank the DGI of Spain and the Consejería de Educación de Asturias for financial support (Projects CTQ2006-01207 and IB05-110), and the MEC of Spain for grants (to M.A. and D.G.-V.). We also thank the Universidad de Santiago de Compostela (Spain) for the acquisition of the X-ray diffraction data of compound **7**.

Supporting Information Available: A CIF file containing the crystallographic data for the structural analysis of compounds **3**, **5**, **7**, **8d**, and **9e**, and a pdf file showing the $^{31}P\{^1H\}$ NMR spectra of the crude reaction mixtures leading to the tungsten compounds **4′** and **6**. This material is available free of charge via the Internet at http://pubs.acs.org.